Zooplankton community succession and trophic links during a mesocosm experiment in the coastal upwelling off Callao Bay (Peru)

Patricia Ayón Dejo[1], Elda Luz Pinedo Arteaga[1], Anna Schukat[2], Jan Taucher[3], Rainer Kiko[3,4], Helena Hauss[3,5], Sabrina Dorschner[2], Wilhelm Hagen[2], Mariona Segura-Noguera[6], and Silke Lischka[3,5]

[1]Instituto del Mar del Perú (IMARPE), Dirección General de Investigaciones en Oceanografía y Cambio Climático, Callao, Perú
[2]University of Bremen, BreMarE Bremen Marine Ecology, Marine Zoology, Bremen, Germany
[3]GEOMAR Helmholtz Centre for Ocean Research Kiel, Biological Oceanography, Kiel, Germany
[4]Laboratoire d'Océanographie de Villefranche-sur-Mer, Sorbonne Université, Villefranche-sur-Mer, France
[5]Department of Computer Science, Christian Albrechts University Kiel, Kiel, Germany
[6]Institut de Ciències del Mar (ICM_CSIC), Barcelona, Spain

Correspondence: Silke Lischka (slischka@geomar.de)

Abstract.

The Humboldt Current Upwelling System (HUS) is the most productive eastern boundary upwelling system (EBU) in terms of fisheries yield on the planet. EBUs are considered hotspots of climate change with predicted expansion of mesopelagic oxygen minimum zones (OMZs) and related changes in frequency and intensity of upwelling of nutrient-rich/oxygen-low deep-water. To increase our mechanistic understanding of how upwelling impacts on plankton communities and trophic links, we investigated mesozooplankton community succession as well as gut fluorescence, fatty acid and elemental compositions (C, N, O, P), and stable isotope (δ^{13}C, δ^{15}N) ratios of dominant meso- and microzooplankton representatives in a mesocosm setup off Callao (Peru) after simulated upwelling with OMZ water from two different locations and N:P signatures. An oxycline between 5 and 15 m with hypoxic conditions below $\sim$10 m ($<50\,\mu$L^{-1}) persisted in the mesocosms throughout the experiment. No treatment effects became apparent in the mesozooplankton community composition, but differences in nutrient concentrations established through OMZ water additions were negligible. Copepods and polychaete larvae dominated in terms of abundance and biomass. Development and reproduction of the dominant copepod genera *Paracalanus* spp., *Hemicyclops* sp., *Acartia* sp., and *Oncaea* sp. was hindered as evident from accumulation of adult copepodids but largely missing nauplii. Failed hatching of nauplii in the hypoxic bottom layer of the mesocosms and poor nutritional condition of copepods suggested from very low gut fluorescence and fatty acid compositions most likely explains the retarded copepod development. Correlation analysis revealed no particular trophic relations between dominant copepods and phytoplankton groups. Possibly particulate organic matter with relatively high C:N ratio was a major diet of copepods. C:N ratios of copepods (pooled and species-specific for *Paracalanus* spp., *Hemicyclops* sp.) and polychaetes ranged between $4.8 - 5.8$ and $4.2 - 4.3$, respectively. Stable isotope signatures of copepods varied over time but not between treatments. δ^{15}N was comparatively high ($\sim 13 - 17\,‰$) potentially because the injected OMZ source water was enriched in δ^{15}N as a result of anoxic conditions. Elemental ratios of dinoflagellates deviated strongly from the Redfield ratio. We conclude, that intensification and increased frequency of upwelling and expanding/shoaling OMZs

could severely impact population dynamics and reproductive success of zooplankton communities and, thus, the pelagic food web of the HUS.

25 **1 Introduction**

Among the four major eastern boundary upwelling systems (EBUSs) the Humboldt Current System (HCS) is the most productive in terms of fisheries yield-. Despite only moderate primary production rates compared with the other EBUSs, the HCS sustains extraordinarily large pelagic fish stocks (Bakun and Weeks, 2008; Chavez et al., 2008). About 10 % of global fish landings originate in the HCS, where more fish per unit area are produced than in any other region in the world due to the

30 fertilizing effect of wind-driven upwelling of cold nutrient-rich waters to the sunlit surface (Chavez et al., 2008). Such an extraordinary high fisheries yield especially off Peru results from a high trophic transfer efficiency that clearly stands out from the other EBUSs (Chavez and Messié, 2009).

Zooplankton play the key role in the transfer of biomass from the primary production level to pelagic fish. Particularly in the northern HCS, upwelling and productivity dynamics are reflected in a close bottom-up driven relationship with the Peruvian

35 anchovy (*Engraulis ringens*), the most important exploited planktivorous fish in that region, although on local scales, top-down regulation of zooplankton by anchovy can occur. Accordingly, changes in zooplankton biomass and composition have direct consequences for higher trophic levels, e.g. fish, seabirds and marine mammals (Ayón et al., 2008b, 2011; Aronés et al., 2019).

Moreover, the HCS is characterized by a uniquely shallow and intense (acidic) oxygen minimum zone (OMZ). In consequence, due to massive loss and source processes of dissolved inorganic nitrogen (N) and phosphorus (P), respectively (Ingall

40 and Jahnke, 1994; Kalvelage et al., 2011), water masses with N:P ratios substantially below the canonical Redfield ratio are upwelled into the surface layer (Franz et al., 2012a; Löscher et al., 2016). Changes in N:P of upwelled water have major impacts on total phytoplankton biomass (Franz et al., 2012b) as well as community structure and fatty acid composition (Hauss et al., 2012), with unclear consequences for consumers. In the course of global climate change, the OMZ will further expand and intensify with severe implications for biogeochemical cycles and pelagic life (Stramma et al., 2008; Schmidtko et al., 2017).

45 On the shelf, the zooplankton community in the Peruvian upwelling region is dominated by small-sized herbivorous copepods that take advantage of phytoplankton blooms developing in the freshly upwelled waters (Espinoza and Bertrand, 2014). With further distance from shore and decreasing primary production, typical slope and oceanic communities are dominated by larger euryphagous or carnivorous organisms such as large copepods, euphausiids and gelatinous plankton (Ayón et al., 2008a). This high offshore zooplankton biomass provides rich feeding grounds for Peruvian anchovy that primarily feed on

50 euphausiids and large copepods (Schwartzlose et al., 1999; Espinoza and Bertrand, 2008; Espinoza et al., 2009; Aronés et al., 2019).

The fertilizing effect of wind-driven upwelling of nutrient-rich waters to the surface in the HCS is subject to major interannual variations due to recurring El Niño events, when weakening trade winds and increased flow of warm water into the eastern equatorial Pacific hinder upwelling of nutrient-rich deeper water (Karl et al., 1995; Escribano, 1998; Carr, 2001).

55 Also, upwelling intensities of nutrient-rich waters are not directly correlated with primary and secondary production off Peru:

intermediate-strength upwelling favours high zooplankton abundance and biomass particularly in spring (October/November), while too strong or too weak upwelling hampers zooplankton productivity in winter and summer, respectively (Ayón et al., 2008a; Chavez and Messié, 2009; Aronés et al., 2019). Whether climate change will cause wind and, hence, upwelling intensities and patterns in the Pacific to decline or increase is currently not clear (Bakun and Weeks, 2008; Gruber et al., 2012), but

60 according to García-Reyes et al. (2015) wind and thus upwelling in the poleward portions of EBUSs have intensified and this trend will continue in the future.

In the past, high fish production was attributed to pelagic fish feeding directly on phytoplankton, indicating high trophic transfer efficiency (Ryther, 1969; Walsh, 1981). More recent studies revealed the dominance of mostly large zooplankton in the diet of anchovies, i.e. copepods and euphausiids (Konchina, 1991; Espinoza and Bertrand, 2008, 2014), and of smaller

65 copepods, less euphausiids (compared to anchovies) and potentially also some phytoplankton in the diet of Pacific sardine due to their smaller gill rakers (Espinoza et al., 2009). These authors hypothesized that *i*) the exceptionally efficient use of primary production by zooplankton, *ii*) the strong connection between coastal and offshore pelagic ecosystems due to the narrow shelf allowing anchovy to extend their foraging grounds over the shelf break further offshore, where they can feed on large energy-rich copepods and euphausiids, and *iii*) the extreme flexibility of anchovy in its diet and feeding behaviour,

70 provide the foundation for the enormous fish production in the HCS. This clearly emphasizes the key role of zooplankton in the pelagic food web off Peru.

Zooplankton species composition and biomass off Peru vary strongly on short time scales due to advection, peaks of larval production, trophic interactions, and community succession (Ayón et al., 2008a). Zooplankton composition itself is regulated by food quality and composition with times of low primary production favouring euryphagous or carnivorous species, when

75 at the same time herbivorous zooplankton is sparse (Ayón et al., 2008a). In fact, micro- and mesozooplankton seem to control phytoplankton standing stocks over the shelf (Minas et al., 1986; Cullen et al., 1992; Franz et al., 2012a).

With an experimental approach we aimed at improving our mechanistic understanding of the interplay between upwelling processes and coastal plankton dynamics in the northern HCS. Therefore, we performed a large-scale mesocosm experiment in the coastal Peruvian upwelling region near Callao in austral summer 2017. By nature, such a closed-system mesocosm

80 setup excludes advection, thus, it allows focusing on intrinsic factors shaping community and food web dynamics like nutrient availability and species dominance. Our experiment coincided with a concurrent strong coastal El Niño, a situation of generally warmer waters and weaker upwelling conditions that favour small-sized zooplankton occurrence in the coastal upwelling areas (Ayón et al., 2011; Bertrand et al., 2011), and consequently dominated our mesozooplankton community in the mesocosm bags at the start of the experiment. During the 50 days of the experiment, we monitored the zooplankton development in

85 eight mesocosms prior to and after a simulated upwelling event through the addition of deeper water of two different OMZ-influenced subsurface waters to four of the mesocosms. To elucidate plankton dynamics and trophic relationships, we followed the temporal development of the mesozooplankton (MeZP) community in relation to that of phytoplankton, analyzed the fatty acid composition and gut fluorescence of dominant copepods, and determined the stable isotope (SI) and elemental composition (C:N) of dominant zooplankton taxa.

2 Methods

2.1 Experimental design

A detailed description of the mesocosm setup and the experimental manipulation is given in Bach et al. (2020). Briefly, eight KOSMOS mesocosm units (cylindrical 18.7 m long polyurethane bags, 2 m diameter, 54.4 $\pm 1.3\,\text{m}^3$ volume) were deployed on February 23, 2017, close to San Lorenzo Island about 4.5 nm off Callao (12.0555° S, 77.2348° W). Nets (mesh size 3 mm) attached to both ends of the bags prevented larger plankton or nekton from entering the mesocosms during deployment. On February 25 (defined as Day 0), the mesocosms were closed at the bottom with a sediment trap. To simulate upwelling with differing inorganic N:P ratios (i.e., with an extreme and a moderate OMZ signature), deeper water was collected on Day 5 at St. 1 from 30 m depth (12.03° S; 77.22° W) and on Day 10 at St. 3 from 90 m depth (12.04° S; 77.38° W) of the IMARPE time-series transect (Graco et al., 2017), using the 100 m³ deep-water collectors described by Taucher et al. (2017). On Day 11 and Day 12, in each mesocosm ~20 m³ of water was exchanged with deep water collected from St. 3 (mesocosms M2, M3, M6, M7) or St. 1 (M1, M4, M5, M8). Special care was taken to evenly withdraw and respectively inject water from/into corresponding depth ranges of the deep-water bag and mesocosms.

Oxygen minimum zones may reach very close to the surface in the near-coast region off Peru (<10 m) (Graco et al., 2017). To conserve the low O_2 bottom layer in the mesocoms that had established after the addition of low oxygen deep-water over the entire experimental duration, water column stratification was artificially maintained by evenly injecting a concentrated NaCl brine solution into the bottom layers of each mesocosm on Day 13 and Day 33. Otherwise, convective mixing induced through heat exchange with the surrounding Pacific would have destroyed the oxygen minimum layer in the mesocosms. For more details on the exact procedure of water exchange and deep-water injection as well as addition of the brine solution see Bach et al. (2020). According to these authors the mesocosm experiment was subdivided into three main phases: Phase 1 lasted from Day 1 until the OMZ water addition (Day 11/12) and was characterized by a diatom-dominated phytoplankton community, phase 2 started with the OMZ water addition until Day 40 and was characterized by a bloom of the mixotrophic dinoflagellate *Akashiwo sanguinea*, and phase 3 continued from Day 40 until the end of the experiment, when eutrophication by defecating seabirds (guanotrophication) triggered a late phytoplankton bloom in most mesocosms.

2.2 Zooplankton sampling

Mesozooplankton (MeZP) samples were always obtained with an Apstein net of 17 cm opening diameter equipped with a 100 μm net bag. Integrated vertical hauls were taken from 17 m depth of each mesocosm and the Pacific close to the mesocosm field. Due to technical/logistic constraints, regular sampling was not possible before Day 18 and therefore sampling intervals varied between 2 and 7 days until Day 18. From then onwards, regular sampling was performed every 6 days. In total, on ten sampling days two net hauls from each mesocosm and the Pacific were performed (Day 0, 8, 10, 13, 18, 24, 30, 36, 42, 48). One of the net contents of each mesocosm was used for species abundance/biomass determination and one for picking live organisms for later fatty acid and elemental analyses (C, N, P, δ^{13}C, δ^{15}N). Mesozooplankton was sampled in the afternoon between 13:00 and 17:00 (local time). As soon as the abundance net haul was retrieved onboard, zooplankton was quantitatively

rinsed into sample bottles with filtered seawater (100 μm). The second net for live organisms was carefully poured into 5 L sampling containers prefilled with 4 L filtered seawater of ambient temperature to accommodate zooplankton organisms and reduce stress. All net samples were stored in cooling boxes to prevent heating until returning to the laboratory and further processing.

Microzooplankton samples for elemental composition analysis were collected from integrated water samplers (see detailed description of water samplers in Bach et al. (2020)). In total, samples were taken at 12 sampling days (Day 0, 8, 10, 13, 16, 18, 20, 26, 30, 36, 42, 48) from each mesocosm and the Pacific. On the first sampling Day 0, samples were collected from the depth intervals 5–0 m and 17–5 m. From Day 8 onwards, sampling depths were 10–0 m and 17–10 m. Until Day 20, samples were regularly taken from both sampling depth intervals, afterwards only the upper interval (10–0 m) was sampled for microzooplankton.

2.3 Abundance and species determinations

In the laboratory, the net samples taken for abundance/biomass determination of each mesocosm were split in half (Motoda splitter) and one half of each sample was preserved in 4 % formaldehyde-seawater solution for subsequent microscopic species identification and enumeration. The other half was used for ZooScan analyses. The formalin-preserved abundance subsample was split applying the Hunstman Marine Laboratory (HML) beaker technique producing count results of a coefficient of variation of 9–15 % from the effective mean (van Guelpen et al., 1982). Subsequently, aliquots were counted under a stereomicroscope (Nikon SMZ 1270) until at least 50 individuals of the most abundant taxa were counted, rare species/taxa were counted from the whole sample. As usual, zooplankton abundances were calculated assuming 100 % filtering efficiency of the net. However, it is well-known that variation among samples is normally high, due to plankton patchiness and moreover variation is species-/taxon-specific (Wiebe and Holland, 1968).

2.4 ZooScan

For the scanning procedure, samples were split further (Motoda splitter) to ratios between 1:4 and 1:32 to avoid crowding in the scanning chamber. In the laboratory, samples were scanned on an Epson Perfection V750 Pro scanner in a modification of the ZooScan method (Gorsky et al., 2010) and a scan chamber constructed of a 21 cm by 29.7 cm (DIN A4) size glass plate with a plastic frame. Scans were 8 bit greyscale, 2400 dpi images (tagged image file format; *.tif). The scan area was partitioned into two halves (i.e. two images per scanned frame) to reduce the size of the individual images and facilitate the processing by ZooProcess/ImageJ. "Vignettes" and image characteristics of all objects were extracted with ZooProcess (Gorsky et al., 2010) and sorted sequentially by first clustering and naming using MorphoCluster (Schröder et al., 2020) and then predicting the remaining unsorted images using deep-learning features in Ecotaxa (http://ecotaxa.obs-vlfr.fr/, Picheral et al. (2017)). Automated image sorting was manually validated by experts. Individual biomass was derived from the image area of each object using published taxon-specific relationships (Lehette and Hernández-León, 2009).

2.5 Zooplankton grazing, gut fluorescence

155 Grazing rates of the dominant copepods *Paracalanus* spp. were analyzed with the gut fluorescence method via experimental determination of gut clearance rates (clearance coefficient) ~~(Mackas and Bohrer, 1976)~~. Clearance rate determination assumes that maximum gut fullness of organisms equals initial gut pigment in the gut clearance experiment (time point zero minutes, $T_{0\,min}$). The experimental identification of a clearance coefficient is accomplished through fluorescence determination of organisms' guts allowed for clearance over a series of time steps for a total period of ca. 1 h. At least eight time steps along the

160 time axis are recommended. Hence, pre-determination of in situ daily maximum gut fullness is required, if maximum ingestion rates are to be estimated (Båmstedt et al., 2000).

Copepods often have diel feeding rhythms (Mackas and Bohrer, 1976). Therefore, prior to clearance rate determination of mesocosm copepods, the feeding rhythmicity and time of maximum gut fullness of dominant copepods (*Paracalanus* spp.) were examined twice over a 24 h cycle, both of copepods collected in the adjacent Pacific as well as of copepods collected in the

165 mesocosms. Each time zooplankton net samples were taken, dominant adult female copepods were picked and ~~gut fluorescence~~ ~~(GF)~~ measured (see below for more details on the procedure). These investigations proved that copepods' feeding activities, i.e. times of maximum gut fullness, were highest at night between approx. 22:55 and 03:40 (Fig. 1). Therefore, sampling of zooplankton in the mesocosms for clearance rate determinations was done at night. It was possible to undertake such attempts during two occasions, during the night of Day 21/22 and during the night of Day 34/35. MeZP samples were collected in all

170 mesocosms with an Apstein net of 17 cm opening diameter equipped with a ~~200~~ μm net bag and a non-filtering cod-end to collect organisms as gentle as possible and prevent stress evacuation of their guts before retrieval of the net.

To determine gut clearance rates and clearance coefficients, immediately after retrieval of each net haul onboard, the zooplankton sample was split in eight subsamples. One of the subsamples was immediately concentrated over a 200 μm mesh, the mesh carefully folded not to squash organisms, wrapped in aluminium foil, and immediately shock-frozen in liquid nitrogen

175 to preserve the in situ-state of gut content upon catch (time-point 0 min, $T_{0\,min}$). The other seven subsamples ($T_{8\,min} - T_{56\,min}$) were incubated in 500 ml filtered seawater each (20 μm) and allowed for gut evacuation over a total period of approximately one hour. After each eight minutes, one of the incubated subsamples was terminated (i.e. last sample after 56 min, $T_{56\,min}$) by concentrating the zooplankton on a 200 μm mesh, the mesh wrapped in aluminium foil and immediately shock-frozen in liquid nitrogen. Back on land, the shock-frozen subsamples of the different mesocosms ($T_{0\,min} - T_{56\,min}$) were stored at –80° C until

180 further processing in the home laboratories in Kiel.

Paracalanus spp. (mostly *Paracalanus parvus*) was the dominating copepod taxon in all mesocosms and therefore was chosen for determination of gut clearance rate. In Kiel, depending on availability, between 8 and 52 individual adult female *Paracalanus* spp. were picked on crushed ice under a stereomicroscope (Wild Heerbrugg M3) from each of the frozen subsamples ($T_{0\,min} - T_{56\,min}$) into 2 ml cryovials placed in a labtop vial cooler at –15° C and at dimmed room light usually within

185 half an hour to prevent destruction of fluorescent pigments (Båmstedt et al., 2000). Loaded vials were stored at –80° C until completion of all samples from all mesocosms. Subsequently, gut pigments were extracted in 1.2 ml 90 % acetone with the help of glass beads (0.5 mm diameter) in a Precellys Evolution HP Homogenizer at 10,000 RPM (9168 g) for 15 sec. Constant
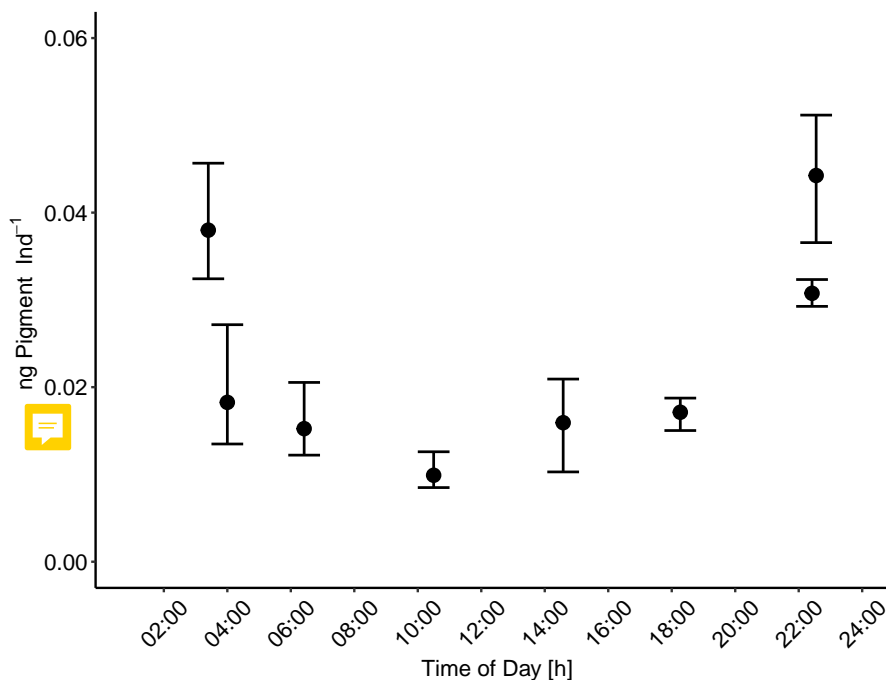
Figure 1. Gut fluorescence: diel feeding rhythm to determine time of maximum gut fullness of adult female *Paracalanus* spp. Gut fluorescence was analyzed on females collected over a 24 h cycle in the mesocosms. Maximum gut fullness was detected early in the morning (03:44) and one hour before midnight (22:55). Error bars are confidence intervals.

cooling of samples was assured during the whole procedure to avoid pigment degradation. After 30 sec of pause, the crushed samples were treated in a Sigma 3–18K centrifuge for 10 min at 10,000 RPM (9168 g) at 4° C to separate liquid and solid

190 phase. Finally, the liquid phase was filtered through 0.2 μm PTFE filters to remove any remaining solid body parts. GF was then measured with a Trilogy Laboratory Fluorometer (Turner Design, USA). The relative fluorescence of each sample was measured three consecutive times and converted to absolute values (ng pigment μg DM^{-1}) by means of a chlorophyll standard curve. To eliminate background fluorescence caused by astaxanthin carotenoids in copepod tissues, GF was corrected by such measured of female *Paracalanus* spp. collected in the surrounding Pacific and starved for 24 h to allow animals to empty their

195 guts completely (Mackas and Bohrer, 1976). An exemplary sample was analyzed for gut pigments (or their degradation products) also by means of reverse phase high performance liquid chromatography (HPLC, Barlow et al. (1997)) calibrated with commercial standards.

To be able to normalize gut fluorescence, dry mass (DM) of female *Paracalanus* individuals was determined of each timepoint subsample. To this end, individual female copepods were picked for DM determination of each sample in triplicate (if

200 enough organisms were available). Additionally, of the Day 21/22 samples females were picked for some C:N determinations usually from $T_{0\,min}$ and $T_{56\,min}$ (13 – 38 individuals per sample depending on availability). Organisms picked for DM determination were rinsed in MilliQ, transferred into pre-weighed tin cups before drying at 60° C for 24 h and mass determinations on

a Mettler Toledo XP2U Ultra Micro Balance (accuracy: 0.000058 – 0.0034 μg). Carbon and nitrogen elemental analyses were done on a Euro EA – CHNSO Element Analyzer according to Sharp (1974).

2.6 Fatty acid analysis of dominant copepods

As soon as possible after collection, adult females of the dominant copepods *Paracalanus* spp. and *Hemicyclops* sp. were picked for lipid analysis from the second net (for live organisms). Due to the high expenditure of time, female copepods were only picked of six mesocosms (M2, M3, M6 of the moderate treatment, M1, M4, M5 of the extreme treatment). Because of limited occurrence during phase 1 and 2 of the experiment, lipid samples of female copepods from the adjacent Pacific could only be picked during phase 3. If available, up to 80 individuals of each species were sorted to assure sufficient lipid mass above detection limit. Some samples were directly transferred to dichloromethane:methanol (2:1, v/v) in 8 ml analytical vials equipped with teflon-sealed screw caps, and some were transferred to Eppendorf caps without solvent. The latter allowed for determination of dry mass (DM) after lyophilization. DM of specimens directly stored in dichloromethane:methanol (2:1, v/v) could not be determined. Samples were stored at –80° C until further analysis in the home laboratory at Bremen University.

DM of the copepods was determined after lyophilization for 48 h (CHRIST Alpha). Total lipids were extracted from the samples after Folch et al. (1957) and Hagen (2000) with dichloromethane:methanol (2:1 v/v). For quantification of total fatty acids (TFA) tricosanoic acid (23:0) was added as an internal standard prior to extraction and TFAs were expressed as the percentage of fatty acids in relation to the dry mass of the sample (TFA % DM). In case of *Paracalanus*, TFAs were related to mesocosm-specific mean DM of females used for gut fluorescence determination, because DM determined after lyophilization of lipid samples was inaccurate. Lipid extraction of samples stored in solvent followed the same procedure as for the lyophilized samples.

Fatty acids were converted to their methylester derivatives (FAME) by transesterification for 4 h at 80° C in hexane and methanol containing 3% concentrated sulphuric acid after Kattner and Fricke (1986). FAMEs were extracted with aqua bidest. and hexane and analyzed by gas chromatography (Agilent Technologies, GC model 7890A). The device was equipped with a DB-FFAP column (30 m length, 0.25 mm inner diameter) and a programmable temperature vaporizer injector, operating with helium as carrier gas (Peters et al., 2007). Fatty acid and alcohol components were detected using a flame ionization detector (FID) and identified by their retention times in comparison to known fatty acid and alcohol standard compositions (FAMEs and free alcohols of the copepod *Calanus hyperboreus* and Supelco 37 Component FAME Mix). In some cases, the lipid mass was very low with a stronger impact of impurities, so that gas chromatography did not result in reliable data. Therefore, data presented here are those that have at least 70% purity of fatty acids relative to impurities. The fatty acid compositions were evaluated according to the fatty acid trophic marker (FATM) concept of Dalsgaard et al. (2003).

2.7 Elemental composition (C, N, P) and stable isotope (δ^{13}C, δ^{15}N) signatures of mesozooplankton

Bulk samples of copepods or polychaetes were used for the analysis of stabile isotope signatures (δ^{13}C and δ^{15}N) and carbon (C), nitrogen (N) and particulate organic phosphorus (POP) content. Copepod samples mainly contained the taxa *Paracalanus* spp. and *Hemicyclops* sp., whereas polychaetes were separated into the species *Paraprionospio* sp. and *Pelagobia longicirrata*.

Copepods and polychaetes were pipetted through a 55 μm nylon mesh attached to a polypropylene tube of $\sim$2 cm length, so that the organisms remained on the mesh. Organisms were shortly rinsed with MilliQ water. Bulk samples were transferred to pre-weighed tin capsules (5x9 mm, Hekatech) and dried at 60° C for at least 24 h. After drying, tin capsules were closed at the top and stored in a 96 well plate covered with Parafilm. In the home laboratories samples were dried again and weighed on a microbalance. Subsamples for phosphorus were taken, whenever enough biomass of the sample was available. Target sample masses were 1 – 4 mg for C:N and 1 – 10 mg for POP. Stable isotopes (^{13}C and ^{15}N), C and N contents were analyzed at the UC Davis Stable Isotope Facility using a PDZ Europa ANCA-GSL elemental analyzer interfaced to a PDZ Europa 20-20 isotope ratio mass spectrometer (Sercon Ltd., Cheshire, UK) with helium as carrier gas. Vienna Pee Dee Belemnite and atmospheric air were used as standards to determine the carbon and nitrogen ratio, respectively. Stable isotope ratios are reported with reference to a standard and expressed in parts per thousand (‰) according to the formula $\delta^{H}X = [(R_{SAMPLE} / R_{STANDARD})]$, where X is the respective element, H gives the heavy isotope mass of that element, and R is the ratio of the heavy to the light isotope.

POP was determined photometrically on a Hitachi U-2900 Spectrophotometer as orthophosphate after oxidative decomposition by adding a spatula tip Oxisolv® 5 ml Milli-Q and the sample in Pyrex tubes and autoclaving. After cooling to room temperature, a subsample (dilution 1:5 or 1:10) was measured according to Ehrhardt and Koeve (1999).

2.8 Elemental composition (C, N, P) of microzooplankton

Samples for X-ray microanalysis (XRMA) were prepared following Segura-Noguera et al. (2012). 500 mL water samples were taken from each mesocosm and the Pacific Ocean and were pre-filtered through a 200 μm nylon mesh to remove larger mesozooplankton. Microzooplankton cells were concentrated via inverse filtration (vacuum pump, 15 μm nylon mesh) to a volume of approximately 2–4 ml. These remaining water samples were pipetted through a 15 μm nylon mesh, so that the organisms remained on the mesh, where they were rinsed several times with ice-cooled Milli Q brought to pH of 8.3–8.5 with NaOH. The last $\sim$50 μl were pipetted to a slide (in several drops) and checked under a stereomicroscope for organisms. 5 μl were transferred to a TEM grid (coated with a formvar carbon film on Copper on 75 mesh, Agar Scientific) in triplicates and again shortly checked under the stereomicroscope to ensure that there was a sufficient number of organisms from the same species to be analyzed. TEM grids were air-dried for about 1 h and afterwards transferred to TEM grid storage boxes and stored in a desiccator container (Fisherbrand™ Circular Bottom Desi-Vac™ Container, Fisher Scientific) until arriving in the home laboratories in Germany. Samples were then kept in vacuum bags until final analysis.

XRMA analysis were done at the Joseph Banks Laboratories in Lincoln, UK. Single cells of microzooplankton were imaged and analyzed for C, N, O, and P elemental content in a FEI Inspect Scanning Electron Microscope (SEM), equipped with an energy-dispersive spectrometer Oxford X-Act silicon drift detector (SDD). X-ray spectra were acquired from an area that circumscribe the cell, at 20 kV of accelerating voltage, accumulation time of 120 sec (life time), spot size 6.0, and 10 mm working distance. Following the analysis of each cell, a blank spectrum (i.e. formvar only) close to the cell was acquired for 30 sec lifetime. Spectra from cells that drifted, changed shape or charged during analysis were discarded. An image before and after the analysis was taken using the INCA Oxford EDS software and the area of analysis was calculated with a MATLAB

270   routine. X-ray bremsstrahlung from each spectrum was removed using NIST DTSA-II Jupiter 2017-11-06 and the intensity of
each peak was also calculated with a MATLAB routine. The standards used for quantification were latex beads of 3 and 5 μm
for C and ADP for N, O and P. Latex beads of 3 μm were analyzed as internal standards several times during each analysis
session to correct for drift and for changes in day-to-day beam intensity. A detailed description of the measuring approach is
given in Segura-Noguera et al. (2016).

2.9   Data evaluation, statistical analysis

Because of the restricted data set with unequal (only samples with 70 % purity) and moreover low numbers of replicates, we
refrained from applying more comprehensive statistical analyses of the lipid data. Instead, we present percentages of total fatty
acid compositions of experimental phase means for each of the studied female copepods together with their 95 % confidence
intervals (CI) to infer potential significance (Field et al., 2012). Similar, MeZP abundance is depicted as treatment (mesocosms

280   with moderate and extreme OMZ water addition, respectively) means per sampling day with their 95 % CIs. Due to generally
very low fluorescence in copepods' guts, we only show initial GF values of copepods of each mesocosm and treatment means
with their standard deviations ($\pm$ SD), since clearance rate measurements, thus grazing rate estimations, were not meaningful
(see results).

Pearson correlations of the dominant zooplankton taxa, the copepods *Paracalanus* spp. and *Hemicyclops* sp., with counts

285   of dominant phyto- and microzooplankton groups (diatoms, phytoflagellates, coccolithophores, dinoflagellates, silicoflagel-
lates, ciliates, all in cells L^{-1}) as well as with concentrations of extracted phytoplankton pigments (Chloro-, Dino-, Crypto-,
Prymnesio-, and Pelagophyceae, diatoms, *Synechococcus*, all in μg L^{-1}) and with total chlorophyll a (μg L^{-1}) were performed
to gain insight into food web relations.

Changes in copepod elemental composition were analyzed using a repeated measures ANOVA (rmANOVA) with treatment

290   and sampling day as factors and mesocosm as a random factor. Statistical analyses were computed using R 3.2.3 (libraries nlme
and lattice). For the two polychaete species as well as the microzooplankton, the sampling design was incomplete.

3   Results

3.1   Zooplankton abundance and contribution of taxonomic groups

Variability of the manual counts of total mesozooplankton abundance (Individuals per Liter, Ind. L^{-1}) was high between meso-

295   cosms and sampling days. Average total mesozooplankton abundance varied between 6.3 Ind. L^{-1} (CI 3.5) on Day 30 and 52.7
Ind. L^{-1} (CI 14.0) on Day 42 in the moderate-treatment mesocosms, and between 7.2 Ind. L^{-1} (CI 3.3) on Day 30 and 33.9 Ind.
L^{-1} (CI 30.1) on Day 42 in the mesocosms with the extreme treatment. Total abundance of mesozooplankton sampled in the
adjacent Pacific was in a similar range as numbers found in the mesocosm treatments (9.7 – 129.3 Ind. L^{-1}) and peaked on Day
48 (Fig. 2). Individual mesocosms developed some more distinct abundance peaks at the beginning and towards the end of the

300   study with maximum numbers of 112.3 Ind. L^{-1} in M1 on Day 10, 127.9 Ind. L^{-1} in M4 on Day 42, and 129.0 Ind. L^{-1} in M3
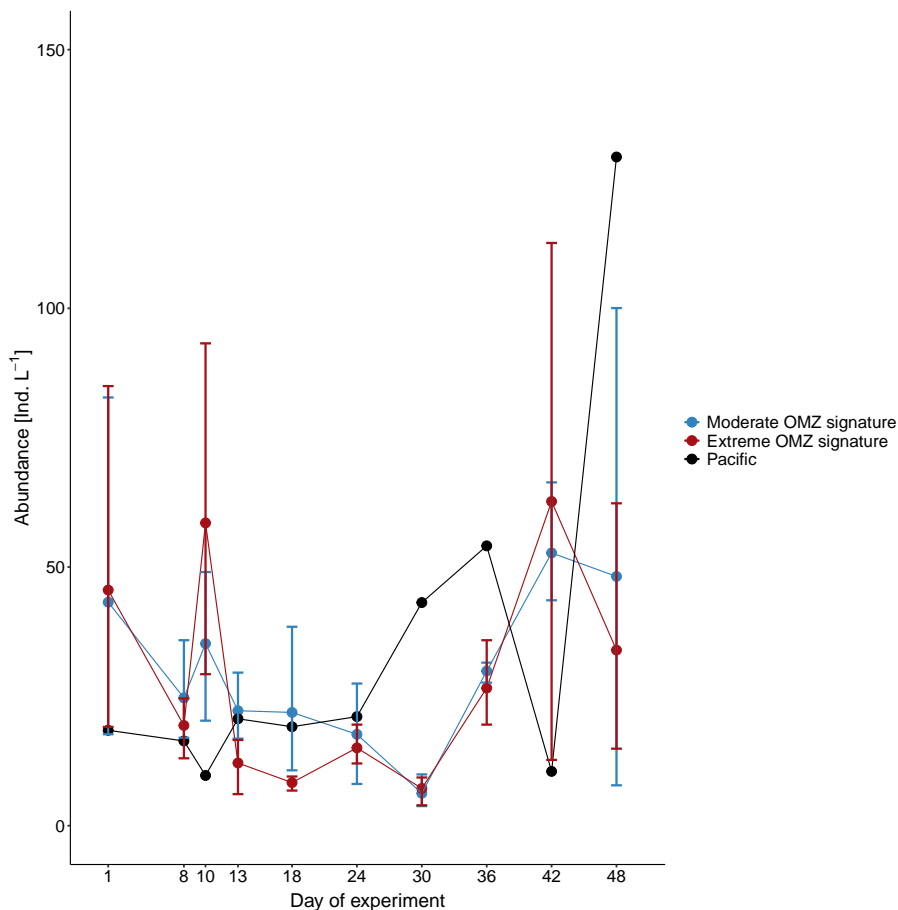
Figure 2. Average total abundance of mesozooplankton (Individuals per Liter, Ind. L^{-1}) in the mesocosms with moderate and extreme OMZ signatures and the surrounding Pacific. Error bars depict 95 % confidence intervals.

on Day 48. Deep-water additions on Day 11 and Day 12 after removal of approx. 20 m^3 of water from each of the mesocosms, respectively (Bach et al., 2020), resulted in distinct deviation from average mesozooplankton abundance between Day 13 and Day 18 with temporarily higher numbers in the moderate mesocosms. This deviation was only short-term and had equalized on Day 24 already, but is indicative of different mesozooplankton densities of the two injected deep-water masses.

305   In terms of abundance, copepods dominated the zooplankton communities at all times both in the mesocosms and the adjacent Pacific. Other taxa (in descending order of contribution: Polychaeta, Echinodermata, Euphausiacea, Mollusca, Hemi-chordata, Cnidaria, Chordata, Cirripedia, Rotifera) contributed only between 0.2% and 18%. Higher shares of other taxa were found only until Day 18, afterwards they were negligible. This pattern essentially reflected the occurrence of copepods and other taxa in the surrounding Pacific (0.3 – 24%), although in the Pacific other taxa contributed higher shares to the zooplankton

310   community after Day 18 (Fig. 3
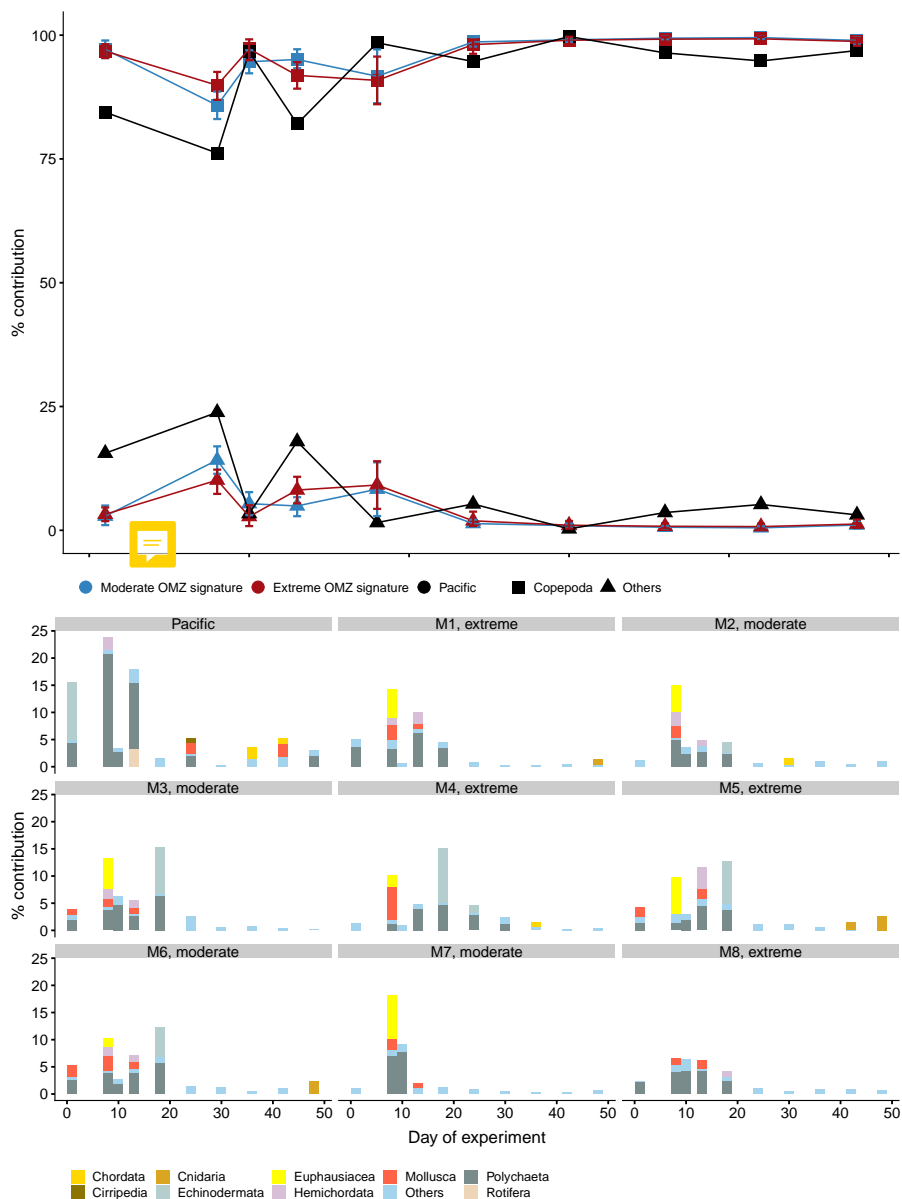
Figure 3. Percent contribution of major taxonomic groups on total mesozooplankton abundance. Upper panel: Copepoda and "Others" (Chordata, Cirripedia, Cnidaria, Echinodermata, Euphausiacea, Hemichordata, Mollusca, Polychaeta, Rotifera). Shown is the mean across OMZ treatments (moderate and extreme signature mesocosms, respectively) with 95% confidence intervals and the contribution of Copepods and "Others" in the Pacific. Lower panel: percent contribution of "Others" shown in the upper panel split into taxonomic groups. Category "Others" summarizes all taxonomic groups that contributed less than 1% on a particular sampling day.

Among other taxa, in the mesocosms, Polychaeta, Echinodermata, Euphausiacea, and Mollusca (taxa ordered in decreasing trend) were most abundant, sometimes constituting more than 5% of total abundance. Remaining taxa consistently contributed less than 5% to total mesozooplankton abundance. Towards the end of the study, the numbers of Chordata (ichthyoplankton) and Cnidaria increased in M1, M2, M4, M5, and M6 to values >1%. In the Pacific in the early phase of the experiment,

315 Polychaeta (up to 21%) and Echinodermata (up to 11%) dominated, followed by Hemichordata (2%) and Rotifera (3%). In the second half of the experiment, Polychaeta, Cirripedia, Mollusca, and Chordata (each <3%) dominated the generally low share of other taxa on total abundance.

3.1.1 Dominant copepods

In terms of relative proportions of total copepod abundance, a species of the cyclopoid genus *Hemicyclops* and species of the

320 calanoid genus *Paracalanus* were the dominant copepods in the mesocosms during the whole experimental duration (Fig. 4). These two genera also prevailed in the adjacent Pacific for most of the time. The genus *Paracalanus* comprised two different species, *P. parvus* and *P.* cf. *quasimodo*. *P. parvus* was numerically dominant and occurred with all copepodite stages. *P.* cf. *quasimodo* was found only in the adult stage, i.e. adult females and males.

In the moderate-treatment mesocosms, the share of *Hemicyclops* sp. varied between 14.2% on Day 48 (CI 4.6) and 65.3%

325 on Day 36 (CI 3.4), and in the extreme-treatment mesocosms between 21.4% on Day 48 (CI 28.6) and 55.9% on Day 13 (CI 20.8). The variability of this genus in the surrounding waters of the Pacific was higher than observed in the mesocosms (74.7% on Day 18, 0.3% on Day 30).

Percent contributions of *Paracalanus* spp. in the moderate-treatment mesocosms ranged between 6.1% on Day 1 (CI 3.7) and 45.7% on Day 42 (CI 30.4), and in the extreme-treatment mesocosms, contributions varied between 12.0% on Day 1 (CI

330 3.7) and 54.0% on Day 18 (CI 17.0). The fractions of this species complex varied in the Pacific between 0.5% on Day 48 and 34.1% on Day 30.

Acartia sp., usually the dominant neritic species in these coastal upwelling areas, was consistently low in the mesocosms with maximum mean portions of around 1% in both treatments. In the adjacent Pacific, contributions ranged between 0.1% and 30.3%.

335 Five different species of the cyclopoid genus *Oncaea* were registered. *Oncaea venusta*, *O.* cf. *chiquito*, and three other *Oncaea* species that could not be identified to species level. *Oncaea* spp. was of some importance in the mesocosms especially in the second half of the experiment, as well as on particular sampling days in the surrounding Pacific.

The cyclopoid genus *Oithona* occurred with four different species, *O. nana*, *O.* cf. *nana* and two undetermined *Oithona* species. Members of the genera *Oithona* had consistently low abundances in the mesocosms but were of minor importance in

340 the second half of the experiment in the Pacific (10.6% on Day 30).

Harpacticoid copepods occurred in the mesocosms in the beginning (44.4% and 33.6% in the moderate and extreme treatment mesocosms, respectively), but decreased quickly after the start of the experiment and continued to have very low shares in both treatments throughout the experiment (≤8%). The succession of harpacticoid copepods in the surrounding Pacific was more variable than in the mesocosms (8 − 33%).
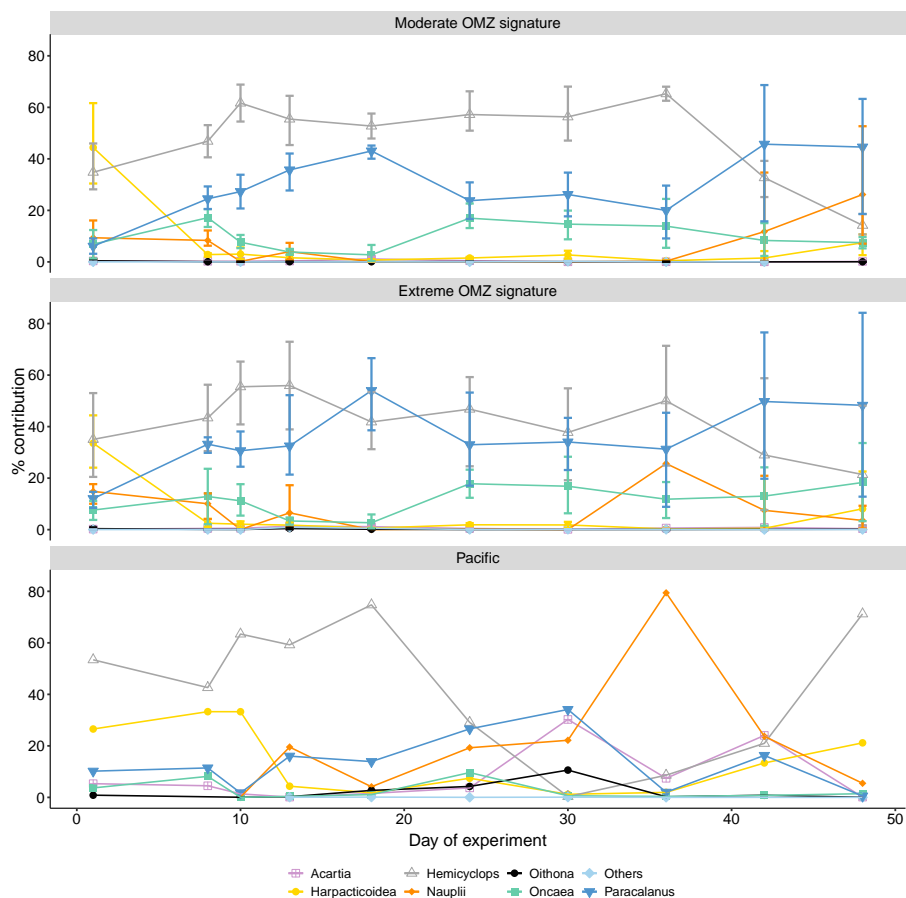
Figure 4. Percent contribution of copepod genus and copepod nauplii on total copepod abundance. Shown is the mean across OMZ treatments (moderate and extreme signature mesocosms, respectively) with 95 % confidence intervals and the contribution of each category in the Pacific. Category "Others" comprises copepods of the genus *Calanus*, *Centropages*, *Clausocalanus*, *Corycaeus*, *Clytemnestra*, *Eucalanus*, *Euterpina*, *Labidocera*, *Mecynocera*, *Microsetella*, *Scolecithrix*, *Temora*.

345   The occurrence of copepod nauplii in the mesocosms was low during most of the experiment. In the moderate treatment, nauplii contributed 9.4% (CI 8.6) on Day 1 and then varied between 4.0% on Day 13 (CI 3.8) and 0% on Day 24. Towards the end of the experiment nauplii increased again to 26.2% (CI 26.8). In the extreme-treatment mesocosms nauplii contribution was 14.8% on Day 1 (CI 4.7) and then varied between 10.1% on Day 8 (CI 6.0) and 3.6% on Day 48 (CI 5.6). An exceptional peak of nauplii was observed in M4 on Day 36 with 25.7% contribution. However, in all mesocosms of the moderate treatment,

350   no nauplii were found on that sampling day. Nauplii contribution in the surrounding Pacific was almost consistently higher than in the mesocosms, except for the first two sampling days, when no nauplii were present in the zooplankton samples. Later on, the share of nauplii varied between 0.1% on Day 10 and 79.4% on Day 36.
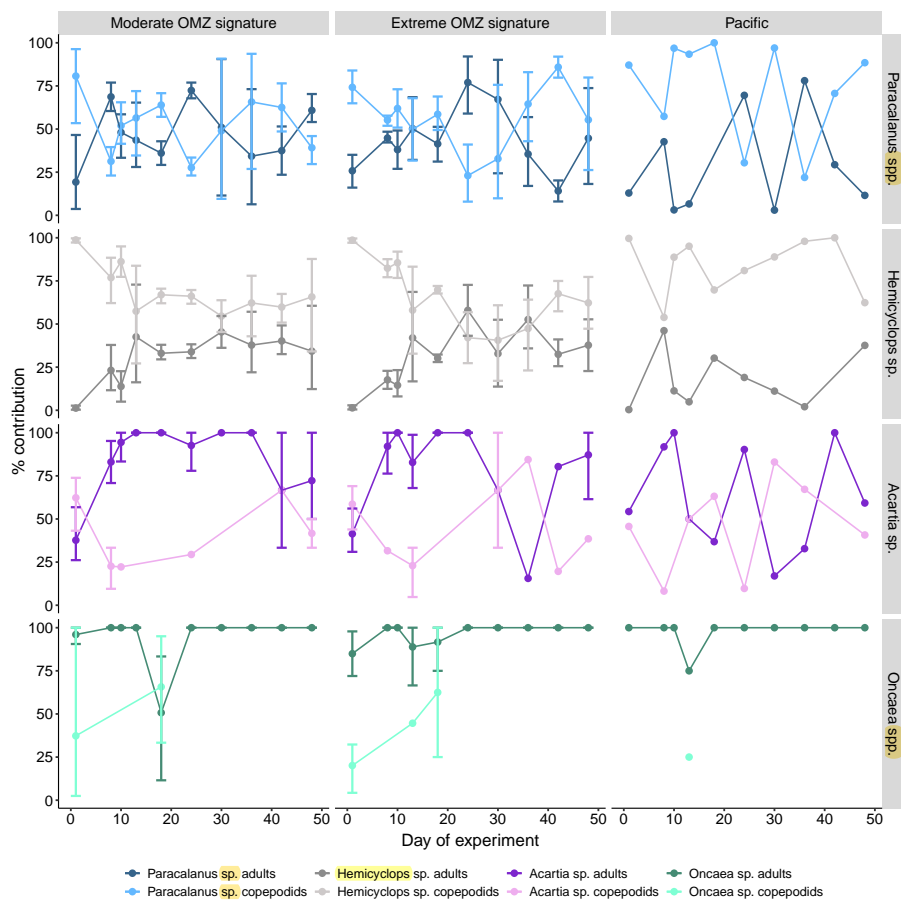
Figure 5. Temporal succession of developmental stages of dominant copepods (average % contribution on total genus abundance with 95% confidence intervals). Adults comprise of female and male copepods, copepodids comprise of stages CI–CV

Copepods of the category "Others" comprised the genera *Calanus*, *Centropages*, *Clausocalanus*, *Corycaeus*, *Clytemnestra*, *Eucalanus*, *Euterpina*, *Labidocera*, *Mecynocera*, *Microsetella*, *Scolecithrix*, and *Temora*. This category accounted on average

355   for less than 1% of total copepod abundance in all mesocosms as well as the Pacific during the whole experiment duration.

3.1.2 Succession of developmental stages of dominant copepods

Figure 5 shows the temporal succession of copepod developmental stages (copepodite stages CI–CV) and of adult copepods (females, males) as percent contribution of total genus abundance for the four major genera *Paracalanus*, *Hemicyclops*, *Acartia*, and *Oncaea*.

360   In general, succession patterns of *Paracalanus* spp. and *Hemicyclops* sp. were similar in both mesocosm treatments. Initially, the percent contributions of adult copepods were low for both genera and copepodids dominated the *Paracalanus* and *Hemicy-*

clops communities, respectively, with on average more than 75% copepodids in both treatments, with a higher variability for *Paracalanus* (larger CIs).

Paracalanus copepodids usually outnumbered adults. Only on Day 8, Day 24, and Day 48 in the moderate treatment and on
365 Day 24 in the extreme-treatment mesocosms, adults accounted for more than 60–70%. The stage contribution of *Paracalanus* in the Pacific was mostly in favour of copepodids (usually >50%), except for Day 24 and Day 36 with >70% adult copepods.

After Day 10, *Hemicyclops* copepodids in the moderate-treatment mesocosms varied between 50% and 65% on average, i.e. the proportion of adults stayed around 35% – 50% for the remaining of the experiment. This relation was similar in the extreme-treatment mesocosms, except that adult copepods exceeded copepodite stages on Day 24 and Day 36 (>50% adults).
370 The portion of *Hemicyclops* copepodids in the surrounding Pacific was consistently higher throughout the experiment and always higher than 50%.

Acartia sp. copepodids dominated in both mesocosm treatments on Day 1 (>50%). Thereafter, the population matured and consisted predominantly of adult copepods. Only on Day 42 and Day 48, copepodids comprised around 70% and 35%, respectively. However, on Day 42, copepodids occurred only in one single mesocosm, as was the case on Day 13 and Day
375 24. The stage distribution of *Acartia* sp. in the surrounding Pacific was more variable. On Day 18, Day 30, and Day 36, the contribution of copepodite stages outnumbered the share of adult *Acartia* sp. (>60%).

Oncaea spp. almost exclusively occurred in the adult stage, both in the mesocosms and the Pacific. Copepodids were only occasionally found with up to >60% contribution.

3.2 Zooplankton biomass

380 Zooplankton biomass (as estimated based upon scanned area of individuals) was dominated by copepods (Fig. 6a), which in the mesocosms ranged between 11.8 and 75.6 μg DM L^{-1} in the first phase, increased to between 8.58 and 137.9 μg DM L^{-1} in the second phase and declined again to between 4.8 and 40.8 μg DM L^{-1} in the third phase. The second most important contributor to zooplankton biomass were polychaetes (Fig. 6b), which in the mesocosms were hardly detected at Day 1 and ranged between 0 and 39.0 μg DM L^{-1} in the first phase, between 0 and 74.7 μg DM L^{-1} in the second phase, and between 0
385 and 0.65 μg DM L^{-1} in the third phase, respectively. M2 and M3 reached biomass maxima both for copepods and polychaetes. In the adjacent Pacific, total copepod and polychaete biomass tended to be lower than in the experimental mesocosms but followed a similar temporal pattern (peaking in phase 2). Among the copepods, the numerically dominant genera *Paracalanus* and *Hemicyclops* were also the main biomass contributors (Fig. 7a and b), with roughly equal share and peaking in phase 2, in particular in the moderate OMZ signature treatments. *Acartia*, which was only present in lower abundance/biomass (Fig. 7c),
390 tended to reach higher biomass in the extreme OMZ signature treatments (in particular in M4). *Oncaea* and other/unidentified cyclopoids (Fig. 7d, f) were mainly present in the first phase 1, with lowest values in phase 2 and a slight increase in phase 3.

In contrast to MeZP abundance, biomass (copepods) peaked between Day 10 and Day 20, but highest abundance values were found towards the end of the experiment when biomass was at a minimum. This discrepancy is most likely due to a shift in the abundance/biomass relationship of dominating zooplankton organisms towards smaller size or lower mass individuals,
395 respectively.
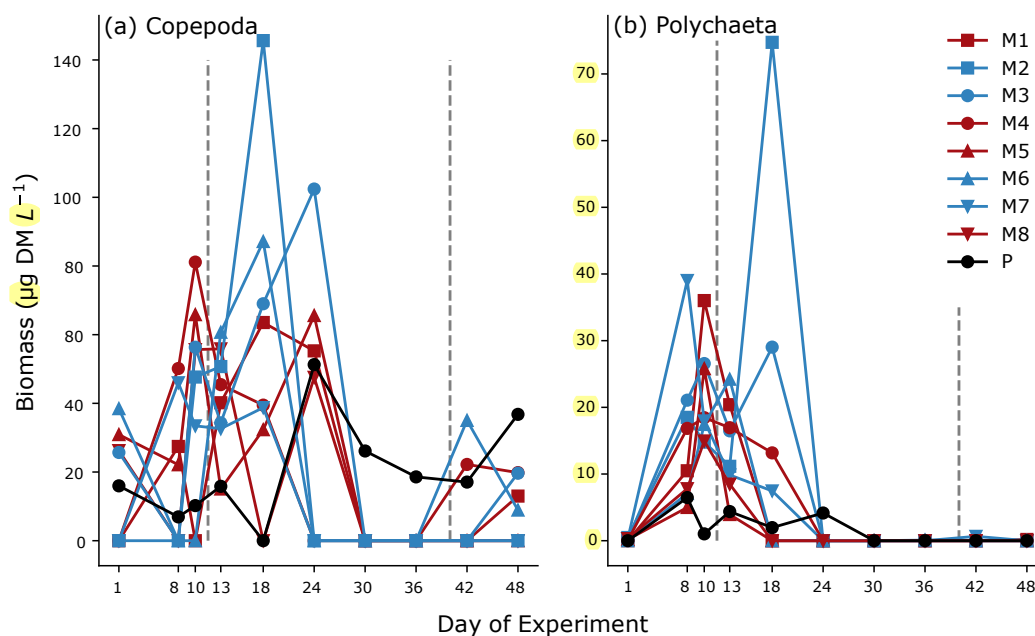
Figure 6. Biomass development (μg DM L^{-1}) over time of total copepods (a) and polychaetes (b) based on image analysis (Zooscan). Vertical dashed lines indicate the three phases according to Bach et al. (2020). Blue = moderate OMZ signature, red = extreme OMZ signature, black = Pacific.

3.3 Zooplankton grazing, gut fluorescence

In general, initial (T$_{0\,\text{min}}$) GF of *Paracalanus* spp. females was low, but treatment averages on Day 34/35 (0.14 and 0.29 ng pigment μg DM^{-1}, respectively) were higher than on Day 21/22 (0.03 and 0.08 ng pigment μg DM^{-1}, respectively), indicating somewhat higher feeding activities of *Paracalanus* females on autotrophic food particles later in the experiment (Table 1). Clearance rate

400 measurements were not meaningful, because GF of incubated copepods showed no clear decreasing trend in GF over time, but GF measured at a later time point was often higher than earlier during the gut evacuation period (data not shown). Frequently, negative values resulted after background fluorescence was subtracted. Such values probably indicated that females had completely emptied their guts during evacuation incubation. However, the high variability between consecutive time intervals impeded meaningful rate estimations. Likely, variability of gut fullness and evacuation of single females of pooled samples

405 was high, preventing successful determination of a decreasing trend with increasing evacuation time. On Day 21/22 female *Paracalanus* of the adjacent Pacific had even lower fluorescence in their guts (0.005 ng pigment μg DM^{-1}) than measured in mesocosm organisms. In contrast to mesocosm organisms, on Day 34/35 there was virtually no fluorescence detectable in females from the Pacific, resulting in a negative GF after background fluorescence was subtracted (-0.004 ng pigment μg DM^{-1}).
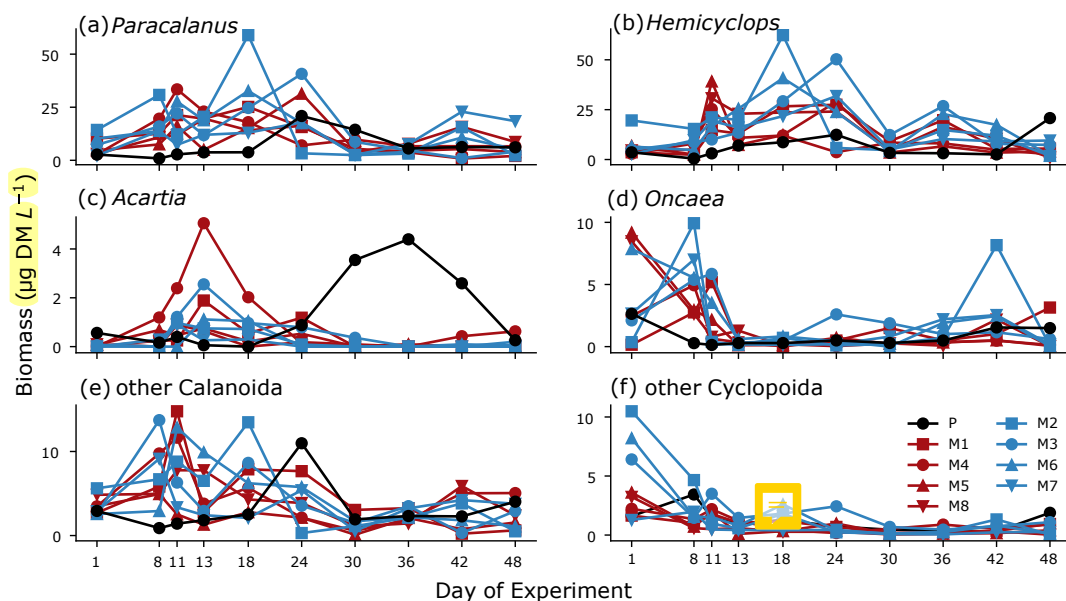
Figure 7. Biomass development of major taxonomic groups during the course of the experiment.

An attempt to analyze gut fluorescence with HPLC to identify degradation products (phaeopigments) of chlorophyll a and

410 conclude on potential food sources (Welschmeyer, 1994) was unsuccessful, probably because of the low GF in the guts of copepods. The chromatogram revealed no identifiable peak(s) besides astaxanthin indicative of the copepods' carapax.

Of copepods collected during the night of Day 21/22, C:N contents (molecular ratios) could be determined and varied between 4.57 and 6.31 across both treatments. Mean values for copepods in mesocosms treated with St. 3 (extreme) and St. 1 (moderate) OMZ water, respectively, were 5.47 ($\pm$ 0.76) and 4.99 ($\pm$ 0.49). Availability of female *Paracalanus* during Day

415 34/35 was not sufficient to reach the detection limit for C:N analysis.

3.4 Lipids

Fatty acid (FA) analyses revealed a relatively high degree of impurities of the samples. This is a common problem in small copepods with rather low total lipid mass close to the detection limit. For this reason, identification of FA peaks in the gas chromatogram was sometimes difficult or even impossible. Therefore, data presented here only include results of samples of

420 which at least 70% of all peaks of a chromatogram could be identified and assigned to a specific FA (i.e. 70% purity).

3.4.1 Total fatty acids

Total fatty acid content (TFA in % DM, equivalent to total lipid levels) of *Paracalanus* spp. (females) from the mesocosms were low (1.5–4.2 % DM) throughout the study period and did not vary significantly between the phases and treatments (Table 2). CIs overlapped, except for the CIs calculated for phase 1 and 3 means of the extreme treatment that suggest more

Table 1. Gut fluorescence (GF) of *Paracalanus* females collected during the night of 18/19 March 2017 (Day 21/22) and during the night of 31 March/01 April 2017 (Day 34/35) immediately frozen after net retrieval onboard to preserve in situ GF (initial gut fluorescence, i.e. $T_{0\,min}$). Standard deviation (SD), C:N values are only available for Day 21/22 and are given as mol/mol.

| | GF (ng pigment μg Dry Mass^{-1}) | | |
| | Day 21/22 | | Day 34/35 |
Mesocosm	Initial	C:N	Initial
OMZ signature of station 3 (moderate)			
2	0.008	5.51 (1.00)	0.207
3	0.090	6.31 (0.05)	0.196
6	–	4.57 (–)	0.099
7	0.018	4.98 (0)	0.052
Mean	0.034 (0.038)	5.47 (0.76)	0.139 (0.075)
OMZ signature of station 1 (extreme)			
1	0.012	4.92 (0.14)	0.014
4	0.089	5.74 (0.12)	0.853
5	0.029	4.57 (0.02)	0.148
8	0.171	4.76 (0.15)	0.156
Mean	0.075 (0.072)	4.99 (0.49)	0.293 (0.380)
Pacific	0.005	5.68 (0.31)	-0.004

425 distinct differences. Mean TFAs of individuals collected in the adjacent Pacific during phase 2 fall within the range of TFA levels determined for the mesocosm copepods. Only one copepod sample from the Pacific could be analyzed in phase 3. This sample had a lower TFA level (0.5 % DM) than those determined for the mesocosm individuals.

During phase 1, *Hemicyclops* sp. was not numerous enough for TFA determination, but it was possible to pick sufficient organisms for lipid analyses during phase 2 and 3. In these two phases, TFA levels of *Hemicyclops* sp. in both treatments
430 ranged between 5.3% DM and 9.3% DM. During phase 3 in the moderate treatment, mean TFA levels were comparatively high (9.3% DM), but did not differ significantly between phases suggesting consistent treatment differences. The TFA level of female *Hemicyclops* sp. collected in the Pacific during phase 2 was lower with 4.7% DM (n=1) than those in the mesocosm *Hemicyclops*. During phase 3, females of *Hemicyclops* sp. from the adjacent Pacific had TFA levels comparable to those of mesocosm females.

Table 2. Fatty acid compositions (% TFA) of females of *Paracalanus* spp. and *Hemicyclops* sp. (mean contributions (%) and confidence limits (CI) of dominant fatty acids as well as the proportions of saturated (SFA), polyunsaturated (PUFA) fatty acids and free fatty alcohols (FAlc). Presented are only data of samples, where the contribution of FAs in relation to impurities was at least 70%. Of those, only FAs are listed, where the phase mean was ⩾2% at least during one occassion. Note: For *Paracalanus* TFA were related to mesocosm-specific average dry mass (DM) of weighed females collected for gut fluorescence; in case of *Hemicyclops* DM could be determined after lyophylization of copepod samples for lipid analysis and was subsequently used for calculation of % TFA.

Phase	FA	*Paracalanus* spp. OMZ signature of St. 1 (M1, M4, M5)	OMZ signature of St. 3 (M2, M3, M6, M7)	adjacent Pacific (field samples)	n (St. 3, St. 1, Pacific)	*Hemicyclops* sp. OMZ signature of St. 1 (M1, M4, M5)	OMZ signature of St. 3 (M2, M3, M6, M7)	adjacent Pacific (field samples)	n (St. 3, St. 1, Pacific)
1	TFA (% DM)	4.2 (±1.5)	3.8 (±0.7)	–	(n = 6, 5, 0)	–	–	–	(n = 0, 0, 0)
2		2.9 (±1.5)	2.3 (±0.7)	1.6 (±1.0)	(n = 13, 4, 2)	5.9 (±0.8)	5.9 (±8.0)	4.7 (–)	(n = 6, 6, 1)
3		1.5 (±1.5)	1.7 (±0.9)	0.5 (–)	(n = 6, 2, 0)	5.3 (±2.0)	9.3 (±4.0)	7.7 (±8.0)	(n = 6, 6, 2)
1	14:0	4.7 (±1.1)	4.7 (±1.0)	–	(n = 4, 4, 0)	–	–	–	(n = 0, 0, 0)
2		3.1 (±0.6)	2.8 (±0.5)	–	(n = 6, 8, 0)	2.1 (±0.1)	2.0 (±0.6)	–	(n = 6, 2, 0)
3		–	2.4 (±0.8)	5.5 (–)	(n = 4, 0, 0)	3.0 (±0.9)	3.1 (±0.9)	1.9 (±0.6)	(n = 3, 4, 2)
1	16:0	17.6 (±1.8)	19.1 (±2.9)	–	(n = 4, 4, 0)	–	–	–	(n = 0, 0, 0)
2		22.5 (±3.2)	20.9 (±3.4)	–	(n = 6, 8, 0)	21.7 (±1.6)	20.3 (±0.8)	–	(n = 6, 2, 0)
3		–	19.7 (±2.4)	23.9 (–)	(n = 4, 0, 0)	24.3 (±5.3)	24.1 (±0.7)	16.7 (±5.0)	(n = 3, 4, 2)
1	16:1(n-7)	5.2 (±2.7)	5.0 (±2.9)	–	(n = 4, 4, 0)	–	–	–	(n = 0, 0, 0)
2		1.2 (±0.3)	1.3 (±0.3)	–	(n = 6, 8, 0)	2.9 (±1.2)	2.7 (±0.6)	–	(n = 6, 2, 0)
3		–	2.0 (±1.0)	10.1 (–)	(n = 4, 0, 0)	2.3 (±0.8)	3.1 (±0.5)	2.9 (±1.9)	(n = 3, 4, 2)
1	18:0	7.0 (±1.9)	7.9 (±2.6)	–	(n = 4, 4, 0)	–	–	–	(n = 0, 0, 0)
2		14.7 (±5.3)	13.6 (±8.0)	–	(n = 6, 8, 0)	9.5 (±2.3)	9.7 (±1.1)	–	(n = 6, 2, 0)
3		–	9.4 (±0.7)	9.2 (–)	(n = 4, 0, 0)	16.1 (±9.8)	8.0 (±1.9)	10.1 (±2.4)	(n = 3, 4, 2)
1	20:5(n-3)	21.7 (±5.9)	20.7 (±5.7)	–	(n = 4, 4, 0)	–	–	–	(n = 0, 0, 0)
2		12.2 (±2.6)	12.4 (±2.6)	–	(n = 6, 8, 0)	7.9 (±0.6)	8.4 (±0.9)	–	(n = 6, 2, 0)
3		–	16.3 (±2.9)	21.0 (–)	(n = 4, 0, 0)	10.3 (±6.6)	8.5 (±0.7)	29.7 (±34.2)	(n = 3, 4, 2)
1	22:5(n-3)	1.4 (±0.3)	0.7 (±0.8)	–	(n = 4, 4, 0)	–	–	–	(n = 0, 0, 0)
2		1.0 (±0.5)	0.0 (±0.0)	–	(n = 6, 8, 0)	1.5 (±0.1)	2.0 (±0.5)	–	(n = 6, 2, 0)
3		–	0.0 (±0.0)	2.4 (–)	(n = 4, 0, 0)	1.1 (±0.8)	0.9 (±0.9)	1.8 (±1.2)	(n = 3, 4, 2)
1	22:6(n-3)/24:1(n-7)	33.4 (±9.1)	34.3 (±4.8)	–	(n = 4, 4, 0)	–	–	–	(n = 0, 0, 0)
2		34.8 (±7.7)	38.5 (±8.2)	–	(n = 6, 8, 0)	47.4 (±5.0)	46.7 (±3.3)	–	(n = 6, 2, 0)
3		–	45.8 (±2.4)	20.9 (–)	(n = 4, 0, 0)	35.0 (±10.5)	46.7 (±2.8)	27.3 (±17.0)	(n = 3, 4, 2)
1	SFA	31.8 (±3.1)	34.2 (±6.0)	–	(n = 4, 4, 0)	–	–	–	(n = 0, 0, 0)
2		43.7 (±8.8)	40.3 (±11.6)	–	(n = 6, 8, 0)	36.3 (±4.5)	35.2 (±1.9)	–	(n = 6, 2, 0)
3		–	33.7 (±3.5)	39.8 (–)	(n = 4, 0, 0)	47.2 (±14.2)	37.8 (±1.8)	31.5 (±10.5)	(n = 3, 4, 2)
1	PUFA	59.8 (±2.3)	58.5 (±7.9)	–	(n = 4, 4, 0)	–	–	–	(n = 0, 0, 0)
2		50.1 (±10.1)	54.0 (±11.3)	–	(n = 6, 8, 0)	58.2 (±5.2)	58.6 (±3.3)	–	(n = 6, 2, 0)
3		–	62.4 (±2.8)	48.4 (–)	(n = 4, 0, 0)	47.4 (±13.8)	56.5 (±2.3)	62.0 (±14.6)	(n = 3, 4, 2)
1	FAlc	0.7 (±0.7)	0.6 (±1.1)	–	(n = 4, 4, 0)	–	–	–	(n = 0, 0, 0)
2		1.9 (±1.6)	1.0 (±0.6)	–	(n = 6, 8, 0)	0.6 (±0.6)	1.3 (±1.2)	–	(n = 6, 2, 0)
3		–	0.5 (±0.1)	0 (–)	(n = 4, 0, 0)	0.9 (±0.4)	0.8 (±1.0)	1.4 (±0.2)	(n = 3, 4, 2)

3.4.2 Fatty acid and fatty alcohol composition

The mean contribution and composition of specific fatty acids (FAs) and fatty alcohols (FAlcs) to total FA and FAlcs of *Paracalanus* and *Hemicyclops* females are presented in Table 2 for the three different experimental phases. Only FAs that reached mean contributions of 2% during at least one of the three phases and the sum of FAlcs were included in the list. Generally, FA and FAlc compositions of both species did not differ much over time and treatment.

Dominant FAs in *Paracalanus* females were 20:5(n-3) and 22:6(n-3)/24:1(n-7), typical biomembrane components. Unfortunately, the peaks of the FAs 22:6 and 24:1 overlapped in the gas chromatogram and could not be separated in all cases, although a dominance of the ubiquitous 22:6(n-3) can be assumed. The mean amount of 20:5(n-3) varied between 12% and 22% TFA, with confidence intervals (CIs) of phase 1 and 2 not overlapping. During phase 3, a lipid sample of *Paracalanus* females from the adjacent Pacific could be analyzed. Those female copepods comprised 21 % of the FA 20:5(n-3), thus similar to phase 1 mesocosm females. The percentage of the 22:6(n-3)/(24:1(n-7) FA was higher in mesocosm females (33–46% TFA) than in females from the Pacific (21% TFA), but did not differ significantly between phases. CIs do not suggest any consistent differences between phases. 16:0 is another important biomembrane component. This FA occurred in higher concentrations (18–24%) during all phases, both in females from the mesocosm and the Pacific, with their CIs always overlapping. Biomarker FAs such as 16:1(n-7) and 18:1(n-7) typical of diatoms were consistently low. 16:1(n-7) ranged between 1% and 5% TFA in mesocosm females, with CIs indicating some higher contribution during phase 1 compared to phases 2 and 3. The single *Paracalanus* sample analyzed from the Pacific revealed a higher amount of 16:1(n-7) with 10% TFA compared to mesocosm individuals. The percentage of 18:1(n-7) was consistently below 1% and is therefore not listed in Table 2. Mean phase contributions of all other FAs were usually below 10% TFA, except for 18:0 with up to 15% during phase 2, but without significant treatment differences.

Saturated fatty acids (SFAs), polyunsaturated fatty acids (PUFAs) and fatty alcohols (FAlcs) occurred in quite stable proportions over the whole experimental period. Due to the dominance of biomembrane FAs, the amount of PUFAs was consistently higher than that of SFAs, both in females from the mesocosms and the Pacific ranging between 50% and 60% for the first group and 32% to 44% for the latter group. FAlcs were only detected in small amounts between 0.5% and 2% TFA in mesocosm females of *Paracalanus* and were not identified in *Paracalanus* females collected in the Pacific.

The FA signature of *Hemicyclops* females was similar to that of *Paracalanus*. The biomembrane FAs 16:0, 20:5(n-3), and 22:6(m-3)/(24:1(n-7) dominated. The portion of 16:0 varied between 20% and 24% TFA in mesocosm females and was somewhat higher than in females collected in the Pacific (17%). The mean contributions of 20:5(n-3) ranged between 8% and 10% TFA in mesocosm females, while in females from the Pacific this FA comprised 30% TFA. 22:6(n-3)/(24:1(n-7) ranged from 35 to 48% TFA in mesocosm females and contributed 28% TFA in females collected in the Pacific. The share of the diatom biomarker FAs 16:1(n-7) and 18:1(n-7) was very low, between 2% and 3% TFA in case of 16:1(n-7) and below 2% TFA for the latter (and therefore not listed in Table 1). Of the remaining FAs, only 18:0 reached contributions between 9% and 16%, all others were below 3% TFA. Only in the case of 22:6(n-3)/24:1(n-7) during phase 3 the CIs did not overlap. These females

from the moderate treatment had somewhat higher shares of that FA compared to females of the other treatment and from the Pacific. However, due to the incomplete separation of these two FAs, we do not consider this result as particularly robust.

470   PUFAs, mainly 20:5(n-3) and 22:6(n-3)/24:1(n-7), of female *Hemicyclops* and *Paracalanus* ranged between 50% and 62% of TFA in the mesocosms and between 48% and 62% in females collected in the adjacent Pacific. Both species had lower portions of SFAs than PUFAs contributing between 32% and 48% of TFA in copepods of the mesocoms and 32–40% in those collected in the Pacific. At all times, FAlcs comprised less than 2% of TFA indicating that these females of both genera did not accumulate significant amounts of wax esters (storage lipids).

475   **3.5   Food web relationships**

Pearson correlations (data not shown) revealed no particularly strong relationships between protist groups and adult and copepodite stages of the copepods *Paracalanus* spp. and *Hemicyclops* sp.. The majority of correlations with a higher correlation coefficient were influenced by a single value, thus, we do not consider these correlations meaningful, in spite of their significance. Apart from that, no consistent associations were identified across the single mesocosms or the two OMZ treatments.

480   Some more meaningful positive correlations were determined for both genera with Pelagophyceae, silicoflagellates, total Chl *a*, Cryptophyceae, and Chlorophyceae. More conclusive negative correlations existed with dinoflagellates and Prymnesiophyceae. However, none of these correlations were consistent in all mesocosms, i.e. we could not identify a consistent foodweb relation pattern for the dominant *Paracalanus* and *Hemicyclops* species in the different mesocosms. Apparently, these copepods fed very opportunistically with no major preference for any of the occurring protist groups. In the adjacent Pacific, positive

485   correlations for *Paracalanus* spp. existed with silicoflagellates, Dinophyceae, Chlorophyceae and Chl *a*.

3.6   Stable isotope and elemental composition

δ^{15}N and δ^{13}C values of copepods (bulk samples) were not impacted by treatment (except a marked difference in M4), but varied significantly over time (p<0.0001), with a general increase in δ^{15}N and a decrease in δ^{13}C during the experimental period (Fig. 8).

490   During phase 1, δ^{15}N of copepods increased by $\sim$1‰ in all mesocosms, a further increase of $1-2$‰ in δ^{15}N occurred during phase 2, while copepod δ^{15}N slightly decreased during phase 3. δ^{13}C was highest during phase 1 and fluctuated between phase 2 and 3. In mesocosm M4, the decrease in δ^{13}C was particularly pronounced. Generally, δ^{15}N values were substantially higher and δ^{13}C values slightly lower in the mesocosms than in the copepods from the adjacent Pacific (Fig. 8). Copepod pooled C:N was unaffected by treatment or time, with an average value of 4.8 ($\pm$ 0.2), and ranged between 5.1 and 5.8 for

495   *Hemicyclops* sp. and *Paracalanus* spp., respectively, based on species/genus-specific determinations. For the two polychaete species, temporal patterns of δ^{15}N and δ^{13}C values were difficult to resolve due to incomplete sampling, and did not reveal a consistent pattern. C:N ratios in the two polychaetes were slightly lower than those of the copepods, with 4.3 ($\pm$ 0.44) and 4.2 ($\pm$ 0.44) in *Paraprionospio* sp. and *P. longicirrata*, respectively. DM-specific organic C, N and P contents were also lower in the two polychaetes than in the copepods. In all mesozooplankton groups, C:P and N:P ratios were higher than 200 and

500   40, respectively (Table 3). While the analysis of parallel samples for C:N and P may explain part of the variability in the
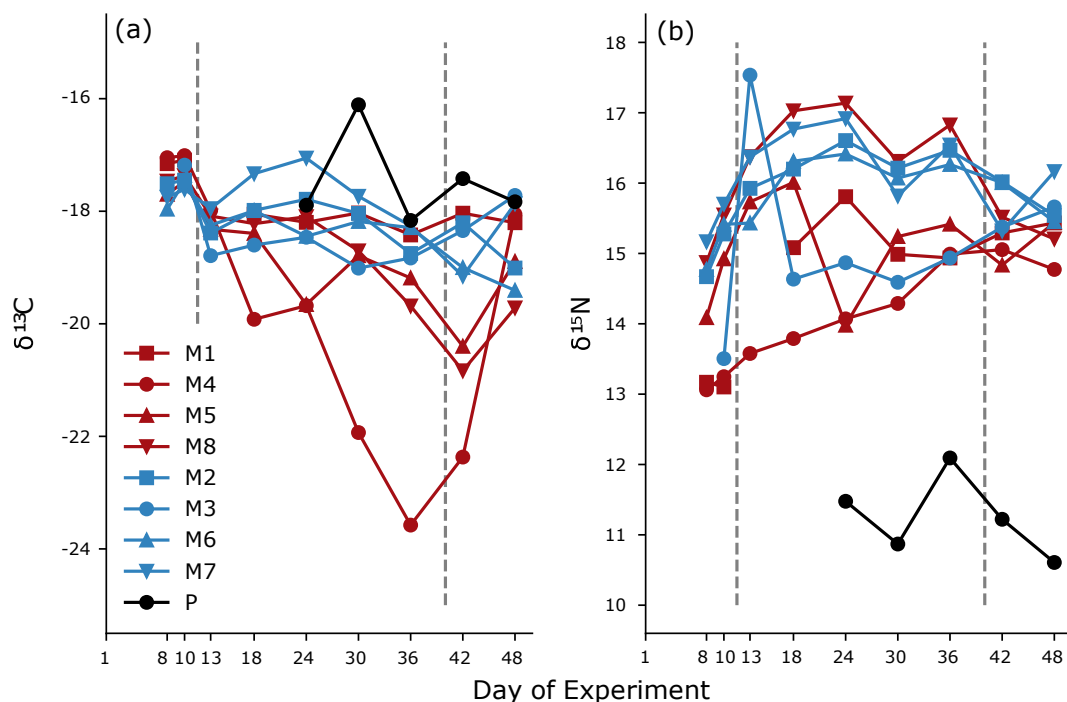
Figure 8. Temporal development of δ^{13}C (a) and δ^{15}N (b) in copepods sampled in the eight mesocosms (M) and the adjacent Pacific (P).

mesozooplankton, the comparatively low P content was also determined in the microzooplankton, where all elemental contents were analyzed per cell. We analyzed microzooplankton cells of the genera *Dinophysis* cf. *punctata* (n = 127), *Tripos* (e.g. *T. fusus*, *T. furca*, n = 25), and *Protoperidinium* sp. (n = 3). In the analyzed dinoflagellates, cellular elemental ratios deviated even more from the canonical Redfield ratio (Table 4). Since the N:P additions in the different mesocosms were not very different,

505 we pooled the analysis of microzooplankton per sampling day. Shown in Table 4 are the average elemental contents (pg cell^{-1}) and molar ratios of *Dinophysis* cf. *punctata* cells. Compared to single-cell analysis of the same taxa from the Mediterranean Sea, all species analyzed here had more C, N and O, but similar P contents (Segura-Noguera et al., 2016).

4 Discussion

Our results are discussed in context with concomitant findings obtained during this mesocosm study, especially phytoplankton

510 succession and biogeochemical aspects relevant for zooplankton dynamics such as an oxycline in the mesocosms between 5 and 15 m with hypoxic conditions at depth (<50 μmol L^{-1}) (Bach et al., 2020). Briefly, phytoplankton composition and successive biogeochemical processes in the mesocosms were driven by a combined influence of N and light limitation (via self-shading of phytoplankton). Bioavailable inorganic N concentrations in the collected OMZ source water were lower than expected. Due to this reason, differences in inorganic N:P signatures established through the addition of OMZ water in the

515 mesocosm treatments were only minor (Bach et al., 2020). Initially, diatoms dominated the phytoplankton communities in the

Table 3. Mean and standard deviation (SD) of dry mass (DM), carbon, nitrogen and phosphorus content of dominant mesozooplankton taxa as well as their molar ratios.

Taxon	DM [μg ind^{-1}]	C [μg mg^{-1} DM]	N [μg mg^{-1} DM]	P [μg mg^{-1} DM]	C:N (molar)	C:P (molar)	N:P (molar)
Copepods (pooled)	NA	338.4 (118.8)	82.9 (28.8)	4.09 (2.14)	4.8 (0.2)	214.4	45.0
Hemicyclops sp., CIV–CV (n=4)	2.2 (0.7)	313.9 (91)	66.5 (19.9)	NA	5.5 (0.15)	NA	NA
Hemicyclops sp., female (n=5)	4.5 (1.2)	404.1 (36.3)	81.1 (6.9)	NA	5.8 (0.11)	NA	NA
Paracalanus spp., CIV–CV (n=4)	3.3. (1.3)	234.4 (94.4)	52.2 (21.3)	NA	5.2 (0.26)	NA	NA
Paracalanus spp., female (n=7)	4.8 (1.7)	254.4 (55.6)	58.7 (13.4)	NA	5.1 (0.17)	NA	NA
Paraprionospio sp.	Na	122.4 (69.6)	32.2 (16.2)	0.74 (1.05)	4.3 (0.44)	424.8	95.7
Paralacydonia longicirrata	NA	117.6 (72)	32.4 (17.2)	1.30 (1.15)	4.4 (0.43)	232.2	53.3

Table 4. Mean and standard deviation (SD) of cellular carbon, nitrogen, oxygen and phosphorus content of dominant microzooplankton taxa.

Species	C [pg cell^{-1}]	N [pg cell^{-1}]	O [pg cell^{-1}]	P [pg cell^{-1}]	C:P (mean)	C:N (mean)	N:P (mean)	C:O (mean)
Ceratium furca	1209 (175)	155 (45)	1072 (316)	5.7 (3.7)	1076.9	9.7	110.4	1.6
Ceratium fusus sp.	1097 (305)	125 (33)	874 (229)	6.5 (2.1)	518.6	10.2	50.4	1.7
Ceratium sp.	2050 (380)	266 (61)	1881 (378)	14.0 (5.2)	453.3	9.2	49.0	1.5
Dinophysis cf. *punctata*	2172 (965)	208 (68)	1460 (463)	9.9 (4.9)	714.3	12.2	61.4	2.0
Protoperidinium sp.	1455 (450)	127 (125)	808 (798)	10.4 (9.3)	502.0	20.2	26.2	3.6

mesocosms. After OMZ deep-water addition and concurrent exhaustion of inorganic nitrogen, the communities shifted towards a pronounced dominance of the mixotrophic dinoflagellate *Akashiwo sanguinea*. Initially ranging between 1.4 and 4.9 μg L^{-1} in the mesocosms, chlorophyll *a* increased only slightly after OMZ water addition to average mesocosm-specific concentrations of max. 5.6 μg L^{-1} between Day 12 and Day 40 without any pronounced peak or treatment separation. Only towards the end of

520 the experiment (after Day 40), eutrophication due to defecating seabirds (guanotrophication) led to an intense phytoplankton bloom and concurrent increase of chlorophyll *a* to values around 20 μg L^{-1} in most mesocosms (Bach et al., 2020).

4.1 Mesozooplankton dynamics

Average total abundance of mesozooplankton (MeZP) was very similar at the start of the experiment and no pronounced differences developed between the two OMZ deep-water treatments over the course of the experiment. The established treatment
525 differences with respect to N:P signatures were significant but small. Phytoplankton community composition was also similar

among all mesocosms, except for M4, which was richer in Cryptophyceae and Chlorophyceae and poorer in Dinophyceae compared to the other mesocosms (Bach et al., 2020). Thus, any potential small-scale treatment differences in MeZP abundance, if existent at all, would have most likely been hidden by methodical uncertainties associated with net sampling, patchy distribution, and counting bias (Algueró-Muñiz et al., 2017; Lischka et al., 2017). For the dominant taxa, the Zooscan method

530 reduces the introduced variability, and adds the size information for each object, allowing biomass estimation. For rare taxa, manual enumeration is to be preferred because of the low split ratios in the scans. The short period of noticeable differences of average abundance between Day 13 and Day 18 can be attributed to the larger water volume added to the extreme-treatment mesocosms during deep-water addition on Day 11 and Day 12 resulting in a stronger dilution effect on the MeZP community compared to that in the moderate mesocosms. This dilution effect had disappeared already on the next sampling day, when

535 abundances were back to similar numbers as in the moderate-treatment mesocosms.

The MeZP community comprised various taxonomic groups with copepods prevailing throughout the experiment both in the mesocosms and the surrounding Pacific, but on average they contributed slightly more to total abundance in the mesocosms. We therefore focus our discussion on this group. All copepod species were pooled in three developmental stages: nauplii, copepodids, and adults. The four main genera were *Paracalanus*, *Hemicyclops*, *Acartia* and *Oncaea*. Species of the genus

540 *Paracalanus*, *Acartia* and *Oncaea* are common in Peruvian coastal and neritic waters (e.g. Ayón et al., 2008a; Aronés et al., 2009; Ayón et al., 2011), whereas the occurrence of the cyclopoid copepod *Hemicyclops* sp. off Callao has only been reported by Criales-Hernández et al. (2008). Generally, the seasonal abundance and distribution of *Hemicyclops* is not well described, but *H. thalassius* comprised a significant portion of the mesozooplankton community in Guanabara Bay, Brazil, similar to the abundance of other common zooplankton organisms (Gomes et al., 2002). The majority of *Hemicyclops* spp. has a symbiotic

545 (commensal, parasitic) lifestyle and occurs on the body surface or in burrows of benthic invertebrates in the intertidal and subtidal zone all over the world except for polar regions (Humes, 1984; Itoh and Nishida, 2008; Korzhavina et al., 2019). Moreover, during their life cycle the majority of *Hemicyclops* spp. changes between a pelagic and a benthic lifestyle with a pelagic phase from nauplius stage NI to the transitional copepodite stage CI and a benthic phase from CI to CIV, when they live associated with the seafloor or the host (Itoh and Nishida, 1995, 2007). *H. thalassius* is the only species of this genus

550 with a holoplanktonic life cycle (Boxshall 1998 cited in Gomes et al., 2002). Thus, we cannot exclude the possibility that *Hemicylops* sp. in the mesocosms were disconnected from their benthic hosts. However, *Hemicyclops* individuals in our study differed from the taxonomic description of the pelagic *H. thalassius* (Vervoort and Ramirez, 1966), therefore we assume a different most likely so far unknown species. *Hemicyclops* sp. regularly occurred in the surrounding Pacific and we found different developmental stages including older copepodids. This together with the fact that the seafloor was mostly anoxic at

555 the mesocosm site during our experiment suggests for a pelagic congener of *H. thalassius*.

Strikingly, copepod nauplii were rare in the mesocosms, particularly after deep-water addition between Day 18 and Day 30 (<1% or absent), although females of the sac-spawning *Hemicyclops* and also the less abundant *Oncaea* were frequently observed carrying egg sacs. In contrast, except for the first days of the experiment, nauplii almost consistently comprised around 20% of all copepod stages in the surrounding Pacific until Day 30 and reached almost 80% on Day 36. This could be explained

560 by advection of copepod populations carrying higher numbers of nauplii (Ayón et al., 2008b) or turbulence/upwelling keeping

eggs in the oxygenated layer and promoting hatching. A lack of nauplii is also reflected in the development of copepodids and adults over the experimental duration and is particularly evident for *Acartia* sp. with adult copepods dominating the population almost over the entire study period. The observed developmental delay of copepodids and adults and especially the very low abundance of nauplii may be a consequence of hypoxic conditions in the mesocosms below ∼10 m. Despite species-specific

565 tolerance levels, copepods generally respond to hypoxic conditions with avoidance (adults) and decreasing rates of survival, egg production and population growth resulting in significant effects on population dynamics (e.g. Judkins, 1980; Marcus et al., 2004; Richmond et al., 2006; Ruz et al., 2017).

Accordingly, maximum abundances of *Paracalanus* cf. *indicus* eggs in Mejillones Bay, Chile, were found in the oxygenated surface waters, whereas egg abundance decreased significantly from the oxygenated layer and the oxycline to the OMZ (Ruz

570 et al., 2017). Sublethal and lethal hypoxia levels (<67 and <31 μmol L^{-1} O$_2$, respectively, Auel and Verheye (2007); Richmond et al. (2006)) occurred in all mesocosms and the surrounding Pacific consistently throughout the study. The oxycline was between 5 and 15 m in the mesocosms and dissolved oxygen concentrations decreased at depth to <50 μmol L^{-1} (Bach et al., 2020). Due to the coastal El Niño, surface temperatures usually varied between 20° C and 22° C, exceptionally reaching 24° C between Day 14 and Day 22. Averaged over the entire water column and all mesocosms, temperatures ranged between

575 18.4° C and 20.2° C from Days 1 to 38 and between 17.9° C and 18.6° C thereafter (Bach et al., 2020). Eggs of *Paracalanus* sp., the dominant broadcast spawning (i.e. eggs released freely into the water column) copepod in the mesocosms, were probably particularly affected by hypoxia, when sinking into low oxygen waters. Sinking velocities of *Paracalanus parvus* eggs determined in the lab and of *P.* cf. *indicus* determined in the field (Mejillones Bay, Chile) ranged between 2.4 – 16.9 m d^{-1} (Checkley, 1980a; Ruz et al., 2017). At a temperature range of 18 – 20° C, *P. parvus* nauplii hatch within 0.40 – 0.46 days

580 and the generation time of *Paracalanus* is about 18 days at 18° C (Checkley, 1980a). Thus, the experimental duration was long enough to expect *Paracalanus* eggs in the mesocosms. Eggs released at the mesocosms' surface would sink to 0.96 – 6.76 m depth within 0.4 days (= 9.6 h), respectively. Eggs released at greater depth would reach the oxycline and hypoxic layers faster, where development was likely halted or eggs may have suffered mortality. This notion is further supported by an accumulation of adults (respectively a minimum contribution of copepodids) around Day 24, after oxygen concentrations in the mesocosms

585 had decreased below 50 μmol O$_2$ L^{-1} below 10 m depth (Bach et al., 2020).

Towards experiment termination, a late increase in copepod nauplii was discernible in the mesocosm treatments on Day 36 (extreme) and Day 42 (moderate). This increase co-occurred with a deepening of hypoxic layers (<55 μmol L^{-1}) from ∼10 m to 14 – 15 m. Similarly, a short intrusion of oxygen-richer waters up to ∼10 m occurred in the adjacent Pacific, parallel to the small nauplii increase on Day 30. Slightly higher oxygen concentrations at the end of the study resulted from a phytoplankton

590 bloom event facilitated through guanotrophication (Bach et al., 2020) and may have supported an increase in eggs and nauplii in both mesocosm treatments.

4.2 Trophic relations

Paracalanus parvus prefers phytoplankton >5 μm over particulate matter as food source, but may also feed on dinoflagellates, when these dominate phytoplankton biomass (Checkley, 1980a; Kleppel and Pieper, 1984). We determined gut fluorescence

595 of *Paracalanus* females during phase 2 of the experiment, when inorganic nitrogen sources were already exhausted and the mixotrophic and facultative osmotrophic dinoflagellate *Akashiwo sanguinea* dominated the phytoplankton community in most mesocosms (absent in M4). In contrast, diatoms dominated in the Pacific almost throughout the study period except for Day 30 and Day 36, when Chlorophyceae, Dinophyceae, and Cryptophyceae prevailed (Kudela et al., 2010; Bach et al., 2020). Visual inspection of guts and measured gut fluorescence of *Paracalanus* females revealed that guts were often empty and

600 that they were not feeding directly on phytoplankton, as gut fluorescence was extremely low. Pigment contents determined for *Paracalanus* in our study were mostly an order of magnitude lower than those of *Acartia*, *Pseudocalanus* and *Temora* from Danish waters (Kiørboe et al., 1985) and of *Acartia* off southern California (Kleppel et al., 1988). This is in accordance with the very low occurrence or absence of phytoplankton biomarker fatty acids determined in *Paracalanus* and *Hemicyclops* females in this study. Due to their very low lipid (TFA) levels, the fatty acid signatures of the copepods analyzed were largely

605 dominated by biomembrane fatty acids (phospholipids), e.g. 16:0, 20:5(n-3) and 22:6(n-3). However, dietary signals of marker fatty acids are conserved in the storage lipids, i.e., in wax esters or triacylglycerols (Lee et al., 2006; Dalsgaard et al., 2003). The marker fatty acid 16:1(n-7) typical of diatoms decreased in *Paracalanus* females from initially ca. 5% to 1 – 2% TFA in phase 3, suggesting diatom ingestion only before or at the beginning of the experiment. On the other hand, *Paracalanus* females collected in the adjacent Pacific during phase 3 had higher 16:1(n-7) concentrations of 10% indicative of diatom

610 feeding in the wild. In contrast, the fatty acid 18:4(n-3) typical of flagellates was not detected in significant amounts in any of the copepods. The near absence of wax esters (storage lipid) agrees with previous studies that egg production in the studied species is related to immediate food supply rather than a period prior to actual egg production, when energy reserves may have been accumulated (Checkley, 1980b). Moreover, of the detected gut fluorescence no clear phaeopigment peaks were identifiable with HPLC, which points to a high degree of degradation of fluorescent pigments found in the guts. Possibly, this

615 'aged' gut fluorescence originated from ingestion of particulate matter, which could also explain why no particularly strong correlations existed between any of the phytoplankton groups and female abundance. The *A. sanguinea* bloom was associated with a marked increase of particulate organic matter and of the C:N ratio (from about 5 – 6 to 8 – 12) in the water column of most mesocosms (Bach et al., 2020). However, phytoplankton availability, respectively dietary nitrogen (i.e. protein), is at times the direct limiting nutrient for egg production of *Paracalanus* (Checkley, 1980b). Hence, nutritional conditions for *Paracalanus*

620 females were apparently insufficient in the mesocosms during phase 2, leading to low egg production and explaining the low numbers of nauplii found in the mesosocoms.

Besides *Paracalanus*, *Hemicyclops* was the other most important copepod genus in the mesocosms that dominated over *Paracalanus* in the moderate mesocosm treatment most of the time. No gut fluorescence could be detected in *Hemicyclops* sp. The fatty acid composition of *Hemicyclops* females was analyzed only from Day 30 onwards and was very similar to that

625 determined for *Paracalanus*. Except for very low concentrations (2 – 3% TFA) of the diatom marker 16:1(n-7), no trophic marker fatty acids were identified and no fatty alcohols were determined, hence, no wax esters (storage lipid) were present. Correlation analysis suggested no particular food preference of *Hemicyclops* for any of the prevailing phytoplankton groups. The diet of *Hemicyclops* species with a coupled pelagic-benthic life cycle consists of micro- and meiobenthos, while detrital particles and also bacteria might be appropriate additional food sources (Itoh and Nishida, 2007, and references therein).

630 Unfortunately, no studies are available on food preferences of *H. thalassius*. Although *Hemicyclops* is an egg-sac spawner, virtually no nauplii were found over the experimental runtime. Using a $100\,\mu$m mesh net, we may have missed the younger nauplii, but should have captured the older naupliar stages (Itoh and Nishida, 2008). From the absence of nauplii despite the frequent presence of egg-sac carrying females, we conclude that the *Hemicyclops* populations in the mesocosms, like *Paracalanus*, also lived at suboptimal conditions, both in terms of nutrition and dissolved oxygen concentrations.

635   Isotopic signatures of zooplankton are determined by source and trophic fractionation. The latter is particularly the case for δ^{15}N, where an increase of $3-4\text{‰}$ per trophic level is usually assumed for marine food webs (Cabana and Rasmussen, 1994; Minagawa and Wada, 1984; Peterson and Fry, 1987). Zooplankton δ^{15}N values ranging approximately between 5 and 13‰ occur in (and close to) upwelling areas (e.g. Rau et al., 2003; Schukat et al., 2014; Teuber et al., 2014), whereas lower zooplankton δ^{15}N values ($\sim 2-4\text{‰}$) were found in regions with high diazotroph contribution to the pelagic food web (Hauss

640 et al., 2013; Sandel et al., 2015). δ^{15}N of zooplankton (copepods) in the mesocosms following a simulated upwelling pulse were rather high ($\sim 13-17\text{‰}$) as compared to the δ^{15}N (mean 7.6‰) measured by Espinoza et al. (2017) for bulk copepod samples of the HCS. The δ^{13}C ratio of copepods from M4 differed profoundly from the other mesocosms in phase 2 (Day 13 – 36). The decrease in δ^{13}C seems to correlate with an increase of Chlorophyceae which made up >90% of the phytoplankton community on Day 36 (Bach et al., 2020). Also, in contrast to the other mesocosms, δ^{15}N was generally lower in M4 in the

645 first two phases. M4 was the only mesocosm lacking the dinoflagellate *Akashiwo sanguinea* (Bach et al., 2020). Mixotrophy by this flagellate could thus have led to increased nitrogen fractionation in the other mesocosms. A comparison of δ^{15}N among different studies without clearly defined baseline values (phytoplankton) for comparison is difficult, as the δ^{15}N baseline is strongly affected by the variability in the intensity of the OMZ along the Peruvian coast (Mollier-Vogel et al., 2012). A recent study by Maßing (2019, master thesis) revealed an enrichment in δ^{15}N of $\sim 5\text{‰}$ for several copepod species of the HCS from

650 north ($8.5°$ S) to south ($16°$ S). The data also showed an increase of δ^{15}N ratios of seston with depth, i.e. between seston from surface oxygenated waters and the OMZ. Dissolved inorganic nitrogen taken up by phytoplankton often creates the basis of the isotopic composition of the whole food web (Argüelles et al., 2012). Under anoxic conditions in OMZs, a preferred uptake of the lighter isotope by denitrifiers leads to elevated δ^{15}N in the remaining nitrate (Granger et al., 2008). OMZs such as the strong and shallow one in the northern HCS are, thus, sites of intense nitrogen loss (Ward et al., 1989) leading to an increase

655 in δ^{15}N baseline values (Sigman et al., 1999; Graham et al., 2010). The higher δ^{15}N of copepods within the mesocosms can therefore be a result of/may be explained by the source water injection to the mesocosms, which was reduced in oxygen and most likely enriched in δ^{15}N.

5   Conclusions

Upwelling is an important factor shaping copepod population dynamics operating through an optimal window of upwelling

660 intensity that fosters copepod abundance and biomass, whereas increasing upwelling may be unfavorable for copepod popula­tions' (Escribano et al., 2012). This is in close connection with the fact that especially smaller copepods such as *Paracalanus* and *Acartia* require well-oxygenated waters for egg development and survival of early-stage copepods for population success

(Ruz et al., 2017). Hence, our findings of failed egg/nauplii development strongly support these earlier notions and underline the importance of mesoscale variability and its implications for copepod reproduction in oxygenated waters and upwelling

665 events, respectively. We conclude that a few meters of oxygenated waters more or less can make a huge difference for copepod secondary production. Therefore, increasing upwelling intensity and shoaling of the OMZ as projected for EBUSs under ocean warming (Stramma et al., 2008; Schmidtko et al., 2017) may have severe consequences for mesopelagic food webs, trophic transfer, and fish production in the HUS (Ayón et al., 2008b; Aronés et al., 2019).

Furthermore, for copepods relying on immediate food supply for egg production, availability of nitrogen-rich food sources is

670 important for reproductive output (Checkley, 1980b). The HUS is characterized by a particularly shallow and pronounced OMZ and enhancement, be it in intensity or expansion, will be accompanied by increasing nitrogen loss processes and upwelling of water masses with N:P ratios below the canonical Redfield ratio (Ingall and Jahnke, 1994; Kalvelage et al., 2011; Franz et al., 2012a; Löscher et al., 2016). Changes in N:P ratios of upwelled water may deteriorate the availability of high-quality (N-rich) nutrition for secondary consumers (Franz et al., 2012b; Hauss et al., 2012) and further contribute to negatively impact copepod

675 reproductive success.

Data availability. All data will be made available on the permanent repository www.pangaea.de after publication. Publication and usage of these data with respect to access and benefit sharing regulations under the Nagoya protocol were approved by the Peruvian Ministry of Production (PRODUCE).

Author contributions. PA, SL, AS, RK, and JT designed the experiment. AS, SL, JT, EP, PA, and RK contributed to the MeZP and MiZP

680 sampling. PA and EP performed MeZP abundance determinations. SL and PA analyzed MeZP abundance data, SL performed correlation analysis. SL collected samples for copepod gut fluorescence, performed analyses, and analyzed data. SL and AS picked copepods for fatty acid analyses, WH and SD performed fatty acid analyses, SL, AS, WH, and SD analyzed fatty acid data. AS performed sampling for SI determinations of MeZP and elemental composition of MiZP, and together with HH and MS-N analyzed the data. JT and RK performed ZooScan analysis, HH analyzed ZooScan data and calculated biomass. SL wrote the manuscript with input from all co-authors.

685 *Competing interests.* The authors declare that they have no conflict of interests.

Acknowledgements. We thank all participants of the KOSMOS Peru 2017 study for assisting in mesocosm sampling and maintenance. We are especially grateful to the IMARPE staff for all support from planning of the study to execution. The captains and crews of BAP Morales, IMARPE VI, and BIC Humboldt are gratefully acknowledged for support during deployment and recovery of the mesocosms and various operations during the course of this investigation. Special thanks go to the Marina de Guerra del Perú, in particular the submarine

690 section of the navy of Callao, and to the Dirección General de Capitanías y Guardacostas. We also thank Club Náutico Del Centro Naval

for hosting and providing laboratory facilities. Our colleagues Clara Beckmann, Jean-Pierre Bednar, Tim Boxhammer, Svenja Christiansen, Lara Durchgraf, Jannik Faustmann, Alba Filella, Marcello Muñiz, Kerstin Nachtigall, Claudia Sforna, Ulf Riebesell, Roberto Quesquén, Laura Schütt, Carsten Spisla, Mayte Tames-Espinosa, Nele Weigt, and Mabel Zavala Moreira are acknowledged for their valuable support during sampling, processing and analyses of zooplankton samples. This project was supported by the Collaborative Research Centre SFB

695 754 Climate-Biogeochemistry Interactions in the Tropical Ocean financed by the German Research Foundation (DFG). Additional funding was provided through the Leibniz Award 2012 granted to Ulf Riebesell. This work is a contribution in the framework of the cooperation agreement between IMARPE and GEOMAR through the German Federal Ministry of Education and Research (BMBF) project ASLAEL 12-016 and the national project Integrated Study of the Upwelling System off Peru developed by the Directorate of Oceanography and Climate Change of IMARPE, PPR 137 CONCYTEC. Rainer Kiko, Silke Lischka, and Helena Hauss received support by the CUSCO project

700 (Bundesministerium für Bildung und Forschung grant no. 03F0813A). Rainer Kiko was further supported via a Make Our Planet Great Again grant of the French National Research Agency within the Programme d'Investissements d'Avenir, reference ANR-19-MPGA-0012.

References

Algueró-Muñiz, M., Alvarez-Fernandez, S., Thor, P., Bach, L. T., Esposito, M., Horn, H. G., Ecker, U., Langer, J. A. F., Taucher, J., Malzahn, A. M., Riebesell, U., and Boersma, M.: Ocean acidification effects on mesozooplankton community development: Results from a long-
705   term mesocosm experiment, PLOS ONE, 12, 1–21, https://doi.org/10.1371/journal.pone.0175851, 2017.

Argüelles, J., Lorrain, A., Cherel, Y., Graco, M., Tafur, R., Alegre, A., Espinoza, P., Taipe, A., Ayón, P., and Bertrand, A.: Tracking habitat and resource use for the jumbo squid *Dosidicus gigas*: a stable isotope analysis in the Northern Humboldt Current System, Marine Biology, 159, 2105–2116, https://doi.org/10.1007/s00227-012-1998-2, 2012.

Aronés, K., Grados, D., Ayón, P., and Bertrand, A.: Spatio-temporal trends in zooplankton biomass in the northern Humboldt
710   current system off Peru from 1961-2012, Deep Sea Research Part II: Topical Studies in Oceanography, 169-170, 104 656, https://doi.org/10.1016/j.dsr2.2019.104656, 2019.

Aronés, K., Ayón, P., Hirche, H.-J., and Schwamborn, R.: Hydrographic structure and zooplankton abundance and diversity off Paita, northern Peru (1994 to 2004) — ENSO effects, trends and changes, Journal of Marine Systems, 78, 582–598, https://doi.org/10.1016/j.jmarsys.2009.01.002, revisiting the Role of Zooplankton in Pelagic Ecosystems, 2009.

715 Auel, H. and Verheye, H. M.: Hypoxia tolerance in the copepod *Calanoides carinatus* and the effect of an intermediate oxygen minimum layer on copepod vertical distribution in the northern Benguela Current upwelling system and the Angola-Benguela Front, Journal of Experimental Marine Biology and Ecology, 352, 234–243, https://doi.org/10.1016/j.jembe.2007.07.020, 2007.

Ayón, P., Criales-Hernandez, M. I., Schwamborn, R., and Hirche, H.-J.: Zooplankton research off Peru: A review, Progress in Oceanography, 79, 238–255, https://doi.org/10.1016/j.pocean.2008.10.020, 2008a.

720 Ayón, P., Swartzman, G., Bertrand, A., Gutiérrez, M., and Bertrand, S.: Zooplankton and forage fish species off Peru: Large-scale bottom-up forcing and local-scale depletion, Progress in Oceanography, 79, 208–214, https://doi.org/10.1016/j.pocean.2008.10.023, 2008b.

Ayón, P., Swartzman, G., Espinoza, P., and Bertrand, A.: Long-term changes in zooplankton size distribution in the Peruvian Humboldt Current System: conditions favouring sardine or anchovy, Marine Ecology Progress Series, 422, 211–222, https://www.int-res.com/abstracts/meps/v422/p211-222/, 2011.

725 Bach, L. T., Paul, A. J., Boxhammer, T., von der Esch, E., Graco, M., Schulz, K. G., Achterberg, E., Aguayo, P., Arístegui, J., Ayón, P., Baños, I., Bernales, A., Boegeholz, A. S., Chavez, F., Chavez, G., Chen, S.-M., Doering, K., Filella, A., Fischer, M., Grasse, P., Haunost, M., Hennke, J., Hernández-Hernández, N., Hopwood, M., Igarza, M., Kalter, V., Kittu, L., Kohnert, P., Ledesma, J., Lieberum, C., Lischka, S., Löscher, C., Ludwig, A., Mendoza, U., Meyer, J., Meyer, J., Minutolo, F., Ortiz Cortes, J., Piiparinen, J., Sforna, C., Spilling, K., Sanchez, S., Spisla, C., Sswat, M., Zavala Moreira, M., and Riebesell, U.: Factors controlling plankton community production, export flux, and
730   particulate matter stoichiometry in the coastal upwelling system off Peru, Biogeosciences, 17, 4831–4852, https://doi.org/10.5194/bg-17-4831-2020, 2020.

Bakun, A. and Weeks, S. J.: The marine ecosystem off Peru: What are the secrets of its fishery productivity and what might its future hold?, Progress in Oceanography, 79, 290–299, https://doi.org/10.1016/j.pocean.2008.10.027, 2008.

Båmstedt, U., Gifford, D., Irigoien, X., Atkinson, A., and Roman, M.: 8 - Feeding, in: ICES Zooplankton Methodology Manual, edited by
735   Harris, R., Wiebe, P., Lenz, J., Skjoldal, H. R., and Huntley, M., pp. 297–399, Academic Press, London, https://doi.org/10.1016/B978-012327645-2/50009-8, 2000.

Barlow, R. G., Cummings, D. G., and Gibb, S. W.: Improved resolution of mono- and divinyl chlorophylls a and b and zeaxanthin and lutein in phytoplankton extracts using reverse phase C-8 HPLC, Marine Ecology Progress Series, 161, 303–307, http://www.int-res.com/abstracts/meps/v161/p303-307/, 1997.

740 Bertrand, A., Chaigneau, A., Peraltilla, S., Ledesma, J., Graco, M., Monetti, F., and Chavez, F. P.: Oxygen: A Fundamental Property Regulating Pelagic Ecosystem Structure in the Coastal Southeastern Tropical Pacific, PLOS ONE, 6, 1–8, https://doi.org/10.1371/journal.pone.0029558, 2011.

Cabana, G. and Rasmussen, J. B.: Modelling food chain structure and contaminant bioaccumulation using stable nitrogen isotopes, Nature, 372, 255–257, https://doi.org/10.1038/372255a0, 1994.

745 Carr, M.-E.: Estimation of potential productivity in Eastern Boundary Currents using remote sensing, Deep Sea Research Part II: Topical Studies in Oceanography, 49, 59–80, https://doi.org/10.1016/S0967-0645(01)00094-7, 2001.

Chavez, F. P. and Messié, M.: A comparison of Eastern Boundary Upwelling Ecosystems, Progress in Oceanography, 83, 80–96, https://doi.org/10.1016/j.pocean.2009.07.032, 2009.

Chavez, F. P., Bertrand, A., Guevara-Carrasco, R., Soler, P., and Csirke, J.: The northern Humboldt Current System: Brief history, present
750 status and a view towards the future, Progress in Oceanography, 79, 95–105, https://doi.org/10.1016/j.pocean.2008.10.012, 2008.

Checkley, D. M.: Food limitation of egg production by a marine, planktonic copepod in the sea off southern California, Limnology and Oceanography, 25, 991–998, https://doi.org/10.4319/lo.1980.25.6.0991, 1980a.

Checkley, D. M.: The egg production of a marine planktonic copepod in relation to its food supply: Laboratory studies, Limnology and Oceanography, 25, 430–446, https://doi.org/10.4319/lo.1980.25.3.0430, 1980b.

755 Criales-Hernández, M. I., Schwamborn, R., Graco, M., Ayón, P., Hirche, H. J., and Wolff, M.: Zooplankton vertical distribution and migration off Central Peru in relation to the oxygen minimum layer, Helgoland Marine Research, 62, 85–100, https://doi.org/10.1007/s10152-007-0094-3, 2008.

Cullen, J. J., Lewis, M. R., Davis, C. O., and Barber, R. T.: Photosynthetic characteristics and estimated growth rates indicate grazing is the proximate control of primary production in the equatorial Pacific, Journal of Geophysical Research, 97, 639–654,
760 https://doi.org/10.1029/91JC01320, 1992.

Dalsgaard, J., St John, M., Kattner, G., Müller-Navarra, D., and Hagen, W.: Fatty acid trophic markers in the pelagic marine environment., Adv Mar Biol, 46, 225–340, https://doi.org/10.1016/s0065-2881(03)46005-7, 2003.

Ehrhardt, M. and Koeve, W.: Determination of particulate organic carbon and nitrogen, chap. 17, pp. 437–444, John Wiley and Sons, Ltd, https://doi.org/10.1002/9783527613984.ch17, 1999.

765 Escribano, R.: Population dynamics of *Calanus chilensis* in the Chilean Eastern Boundary Humboldt Current, Fisheries Oceanography, 7, 245–251, https://doi.org/10.1046/j.1365-2419.1998.00078.x, 1998.

Escribano, R., Hidalgo, P., Fuentes, M., and Donoso, K.: Zooplankton time series in the coastal zone off Chile: Variation in upwelling and responses of the copepod community, Progress in Oceanography, 97-100, 174–186, https://doi.org/10.1016/j.pocean.2011.11.006, global Comparisons of Zooplankton Time Series, 2012.

770 Espinoza, P. and Bertrand, A.: Revisiting Peruvian anchovy (*Engraulis ringens*) trophodynamics provides a new vision of the Humboldt Current system, Progress in Oceanography, 79, 215–227, https://doi.org/10.1016/j.pocean.2008.10.022, 2008.

Espinoza, P. and Bertrand, A.: Ontogenetic and spatiotemporal variability in anchoveta *Engraulis ringens* diet off Peru, Journal of Fish Biology, 84, 422–435, https://doi.org/10.1111/jfb.12293, 2014.

Espinoza, P., Bertrand, A., van der Lingen, C. D., Garrido, S., and Rojas de Mendiola, B.: Diet of sardine (*Sardinops sagax*) in the northern
775   Humboldt Current system and comparison with the diets of clupeoids in this and other eastern boundary upwelling systems, Progress in
     Oceanography, 83, 242–250, https://doi.org/10.1016/j.pocean.2009.07.045, 2009.

Espinoza, P., Lorrain, A., Ménard, F., Cherel, Y., Tremblay-Boyer, L., Argüelles, J., Tafur, R., Bertrand, S., Tremblay, Y., Ayón, P., Munaron,
     J. M., Richard, P., and Bertrand, A.: Trophic structure in the northern Humboldt Current system: new perspectives from stable isotope
     analysis, Marine Biology, 164, 86, https://doi.org/10.1007/s00227-017-3119-8, 2017.

780 Field, A., Miles, J., and Fields, Z., eds.: Discovering Statistics using R, Sage Publications, Ltd, 2012.

Folch, J., Lees, M. B., and Stanley, G.: A simple method for the isolation and purification of total lipids from animal tissues., The Journal of
     biological chemistry, 226 1, 497–509, 1957.

Franz, J., Krahmann, G., Lavik, G., Grasse, P., Dittmar, T., and Riebesell, U.: Dynamics and stoichiometry of nutrients and phytoplankton in
     waters influenced by the oxygen minimum zone in the eastern tropical Pacific, Deep Sea Research Part I: Oceanographic Research Papers,
785   62, 20–31, https://doi.org/10.1016/j.dsr.2011.12.004, 2012a.

Franz, J. M. S., Hauss, H., Sommer, U., Dittmar, T., and Riebesell, U.: Production, partitioning and stoichiometry of organic matter un-
     der variable nutrient supply during mesocosm experiments in the tropical Pacific and Atlantic Ocean, Biogeosciences, 9, 4629–4643,
     https://doi.org/10.5194/bg-9-4629-2012, 2012b.

García-Reyes, M., Sydeman, W. J., Schoeman, D. S., Rykaczewski, R. R., Black, B. A., Smit, A. J., and Bograd, S. J.: Un-
790   der Pressure: Climate Change, Upwelling, and Eastern Boundary Upwelling Ecosystems, Frontiers in Marine Science, 2, 109,
     https://doi.org/10.3389/fmars.2015.00109, 2015.

Gomes, C., Marazzo, A., and Valentin, J.: Occurrence of *Hemicyclops thalassius* Vervoort and Ramirez, 1966 (Copepoda, Poecilostomatoida:
     Clausidiidae) in a tropical bay in Brazil., Nauplius, 10, 77–79, 2002.

Gorsky, G., Ohman, M. D., Picheral, M., Gasparini, S., Stemmann, L., Romagnan, J.-B., Cawood, A., Pesant, S., García-Comas, C.,
795   and Prejger, F.: Digital zooplankton image analysis using the ZooScan integrated system, Journal of Plankton Research, 32, 285–303,
     https://doi.org/10.1093/plankt/fbp124, 2010.

Graco, M. I., Purca, S., Dewitte, B., Castro, C. G., Morón, O., Ledesma, J., Flores, G., and Gutiérrez, D.: The OMZ and nutrient fea-
     tures as a signature of interannual and low-frequency variability in the Peruvian upwelling system, Biogeosciences, 14, 4601–4617,
     https://doi.org/10.5194/bg-14-4601-2017, 2017.

800 Graham, B., Koch, P., Newsome, S., McMahon, K., and Aurioles, D.: Using isoscapes to trace the movements and foraging behavior of top
     predators in oceanic ecosystems, in: Isoscapes: Understanding movement, pattern, and process on Earth through isotope mapping, edited
     by West, J., Bowen, G., Dawson, T., and Tu, K., pp. 299–318, Springer Netherlands, Dordrecht, 2010.

Granger, J., Sigman, D. M., Lehmann, M. F., and Tortell, P. D.: Nitrogen and oxygen isotope fractionation during dissimilatory nitrate
     reduction by denitrifying bacteria, Limnology and Oceanography, 53, 2533–2545, https://doi.org/10.4319/lo.2008.53.6.2533, 2008.

805 Gruber, N., Hauri, C., Lachkar, Z., Loher, D., Frölicher, T. L., and Plattner, G. K.: Rapid progression of ocean acidification in the California
     Current System, Science, 337, 220–223, https://doi.org/10.1126/science.1216773, 2012.

Hagen, W.: ICES Zooplankton Methodology Manual, Elsevier, San Diego, https://doi.org/10.1016/B978-0-12-327645-2.X5000-2, 2000.

Hauss, H., Franz, J. M. S., and Sommer, U.: Changes in N:P stoichiometry influence taxonomic composition and nutritional quality of
     phytoplankton in the Peruvian upwelling, Journal of Sea Research, 73, 74–85, https://doi.org/10.1016/j.seares.2012.06.010, 2012.

810 Hauss, H., Franz, J. M., Hansen, T., Struck, U., and Sommer, U.: Relative inputs of upwelled and atmospheric nitrogen to the eastern tropical North Atlantic food web: Spatial distribution of δ^{15}N in mesozooplankton and relation to dissolved nutrient dynamics, Deep Sea Research Part I: Oceanographic Research Papers, 75, 135–145, https://doi.org/10.1016/j.dsr.2013.01.010, 2013.

Humes, A. G.: *Hemicyclops columnaris* sp.n. (Copepoda, Poecilostomatoida, Clausidiidae) Associated with a Coral in Panama (Pacific Side), Zoologica Scripta, 13, 33–39, https://doi.org/10.1111/j.1463-6409.1984.tb00020.x, 1984.

815 Ingall, E. and Jahnke, R.: Evidence for enhanced phosphorus regeneration from marine sediments overlain by oxygen depleted waters, Geochimica et Cosmochimica Acta, 58, 2571–2575, https://doi.org/10.1016/0016-7037(94)90033-7, 1994.

Itoh, H. and Nishida, S.: Copepodid Stages of *Hemicyclops japonicus* Itoh and Nishida (Poecilostomatoida: Clausidiidae) Reared in the Laboratory, Journal of Crustacean Biology, 15, 134–155, https://doi.org/10.1163/193724095X00640, 1995.

Itoh, H. and Nishida, S.: Life history of the copepod *Hemicyclops gomsoensis* (Poecilostomatoida, Clausidiidae) associated with decapod
820 burrows in the Tama-River estuary, central Japan, Plankton and Benthos Research, 2, 134–146, https://doi.org/10.3800/pbr.2.134, 2007.

Itoh, H. and Nishida, S.: Life history of the copepod *Hemicyclops spinulosus* (Poecilostomatoida, Clausidiidae) associated with crab burrows with notes on male polymorphism and precopulatory mate guarding, Plankton and Benthos Research, 3, 189–201, https://doi.org/10.3800/pbr.3.189, 2008.

Judkins, D. C.: Vertical distribution of zooplankton in relation to the oxygen minimum off Peru, Deep Sea Research Part A. Oceanographic
825 Research Papers, 27, 475–487, https://doi.org/10.1016/0198-0149(80)90057-6, 1980.

Kalvelage, T., Jensen, M. M., Contreras, S., Revsbech, N. P., Lam, P., Günter, M., LaRoche, J., Lavik, G., and Kuypers, M. M. M.: Oxygen Sensitivity of Anammox and Coupled N-Cycle Processes in Oxygen Minimum Zones, PLoS ONE, 6, e29 299, https://doi.org/10.1371/journal.pone.0029299, 2011.

Karl, D. M., Letelier, R., Hebel, D., Tupas, L., Dore, J., Christian, J., and Winn, C.: Ecosystem changes in the North Pacific subtropical gyre
830 attributed to the 1991–92 El Niño, Nature, 373, 230–234, https://doi.org/10.1038/373230a0, 1995.

Kattner, G. and Fricke, H. S.: Simple gas-liquid chromatographic method for the simultaneous determination of fatty acids and alcohols in wax esters of marine organisms, Journal of Chromatography A, 361, 263 – 268, https://doi.org/10.1016/S0021-9673(01)86914-4, 1986.

Kiørboe, T., Møhlenberg, F., and Riisgård, H. U.: In situ feeding rates of plantonic copepods: A comparison of four methods, Journal of Experimental Marine Biology and Ecology, 88, 67–81, https://doi.org/10.1016/0022-0981(85)90202-3, 1985.

835 Kleppel, G. S. and Pieper, R. E.: Phytoplankton pigments in the gut concents of planktonic copepods from coastal waters off southern California, Marine Biology, 78, 193–198, https://doi.org/10.1007/BF00394700, 1984.

Kleppel, G. S., Pieper, R. E., and Trager, G.: Variability in the gut contents of individual *Acartia tonsa* from waters off Southern California, Marine Biology, 97, 185–190, https://doi.org/10.1007/BF00391301, 1988.

Konchina, Y.: Trophic status of the Peruvian Anchovy and Sardine, Journal of Ichtyology, 31, 240–252, 1991.

840 Korzhavina, O. A., Hoeksema, B. W., and Ivanenko, V. N.: A review of Caribbean Copepoda associated with reef-dwelling cnidarians, echinoderms and sponges, Contributions to Zoology, 88, 297 – 349, https://doi.org/10.1163/18759866-20191411, 2019.

Kudela, R. M., Seeyave, S., and Cochlan, W. P.: The role of nutrients in regulation and promotion of harmful algal blooms in upwelling systems, Progress in Oceanography, 85, 122–135, https://doi.org/10.1016/j.pocean.2010.02.008, 2010.

Lee, R., Hagen, W., and Kattner, G.: Lipid storage in marine zooplankton, Marine Ecology Progress Series, 307, 273–306,
845 https://doi.org/10.3354/meps307273, 2006.

Lehette, P. and Hernández-León, S.: Zooplankton biomass estimation from digitized images: a comparison between subtropical and Antarctic organisms, Limnology and Oceanography: Methods, 7, 304–308, https://doi.org/10.4319/lom.2009.7.304, 2009.

Lischka, S., Bach, L. T., Schulz, K.-G., and Riebesell, U.: Ciliate and mesozooplankton community response to increasing CO_2 levels in the Baltic Sea: insights from a large-scale mesocosm experiment, Biogeosciences, 14, 447–466, https://doi.org/10.5194/bg-14-447-2017, 2017.

850

Löscher, C. R., Bange, H. W., Schmitz, R. A., Callbeck, C. M., Engel, A., Hauss, H., Kanzow, T., Kiko, R., Lavik, G., Loginova, A., Melzner, F., Meyer, J., Neulinger, S. C., Pahlow, M., Riebesell, U., Schunck, H., Thomsen, S., and Wagner, H.: Water column biogeochemistry of oxygen minimum zones in the eastern tropical North Atlantic and eastern
tropical South Pacific oceans, Biogeosciences, 13, 3585–3606, https://doi.org/10.5194/bg-13-3585-2016, 2016.

855 Mackas, D. and Bohrer, R.: Fluorescence analysis of zooplankton gut contents and an investigation of diel feeding patterns, Journal of Experimental Marine Biology and Ecology, 25, 77–85, https://doi.org/10.1016/0022-0981(76)90077-0, 1976.

Marcus, N. H., Richmond, C., Sedlacek, C., Miller, G. A., and Oppert, C.: Impact of hypoxia on the survival, egg production and population dynamics of *Acartia tonsa* Dana, Journal of Experimental Marine Biology and Ecology, 301, 111–128, https://doi.org/10.1016/j.jembe.2003.09.016, 2004.

860 Maßing, J.: Food-web structure and trophic interactions in the Humboldt Current upwelling system off Peru, Master's thesis, Bremen, 2019.

Minagawa, M. and Wada, E.: Stepwise enrichment of δ^{15}N along food chains: Further evidence and the relation between δ^{15}N and animal age, Geochimica et Cosmochimica Acta, 48, 1135–1140, https://doi.org/10.1016/0016-7037(84)90204-7, 1984.

Minas, H. J., Minas, M., and Packard, T. T.: Productivity in upwelling areas deduced from hydrographic and chemical fields, Limnology and Oceanography, 31, 1182–1206, https://doi.org/10.4319/lo.1986.31.6.1182, 1986.

865 Mollier-Vogel, E., Ryabenko, E., Martinez, P., Wallace, D., Altabet, M. A., and Schneider, R.: Nitrogen isotope gradients off Peru and Ecuador related to upwelling, productivity, nutrient uptake and oxygen deficiency, Deep Sea Research Part I: Oceanographic Research Papers, 70, 14–25, https://doi.org/10.1016/j.dsr.2012.06.003, 2012.

Peters, J., Dutz, J., and Hagen, W.: Role of essential fatty acids on the reproductive success of the copepod *Temora longicornis* in the North Sea, Marine Ecology Progress Series, 341, 153–163, 2007.

870 Peterson, B. J. and Fry, B.: Stable isotopes in ecosystem studies, Annual Review of Ecology and Systematics, 18, 293–320, https://doi.org/10.1146/annurev.es.18.110187.001453, 1987.

Picheral, M., Colin, S., and Irisson, J.-O.: EcoTaxa, a tool for the taxonomic classification of images, http://ecotaxa.obs-vlfr.fr, 2017.

Rau, G. H., Ohman, M. D., and Pierrot-Bults, A.: Linking nitrogen dynamics to climate variability off central California: a 51 year record based on δ^{15}N/δ^{14}N in CalCOFI zooplankton, Deep Sea Research Part II: Topical Studies in Oceanography, 50, 2431–2447,
875 https://doi.org/10.1016/S0967-0645(03)00128-0, 2003.

Richmond, C., Marcus, N. H., Sedlacek, C., Miller, G. A., and Oppert, C.: Hypoxia and seasonal temperature: Short-term effects and long-term implications for Acartia tonsa dana, Journal of Experimental Marine Biology and Ecology, 328, 177–196, https://doi.org/10.1016/j.jembe.2005.07.004, 2006.

Ruz, P., Hidalgo, P., Riquelme-Bugueño, R., Franco-Cisterna, B., and Cornejo, M.: Vertical distribution of copepod eggs in the oxygen
880 minimum zone off Mejillones Bay (23°S) in the Humboldt Current System, Marine Ecology Progress Series, 571, 83–96, https://www.int-res.com/abstracts/meps/v571/p83-96/, 2017.

Ryther, J. H.: Photosynthesis and Fish Production in the Sea, Science, 166, 72–76, https://doi.org/10.1126/science.166.3901.72, 1969.

Sandel, V., Kiko, R., Brandt, P., Dengler, M., Stemmann, L., Vandromme, P., Sommer, U., and Hauss, H.: Nitrogen Fuelling of the Pelagic Food Web of the Tropical Atlantic, PLOS ONE, 10, 1–19, https://doi.org/10.1371/journal.pone.0131258, 2015.

885 Schmidtko, S., Stramma, L., and Visbeck, M.: Decline in global oceanic oxygen content during the past five decades, Nature, 542, 335–339, https://doi.org/10.1038/nature21399, 2017.

Schröder, S.-M., Kiko, R., and Koch, R.: MorphoCluster: Efficient Annotation of Plankton Images by Clustering, Sensors, 20, https://doi.org/10.3390/s20113060, 2020.

Schukat, A., Auel, H., Teuber, L., Lahajnar, N., and Hagen, W.: Complex trophic interactions of calanoid copepods in the Benguela upwelling
890 system, Journal of Sea Research, 85, 186–196, https://doi.org/doi.org/10.1016/j.seares.2013.04.018, 2014.

Schwartzlose, R. A., Alheit, J., Bakun, A., Baumgartner, T. R., Cloete, R., Crawford, R. J., Fletcher, W. J., Green-Ruiz, Y., Hagen, E., Kawasaki, T., Lluch-Belda, D., Lluch-Cota, S. E., MacCall, A. D., Matsuura, Y., Nevárez-Martínez, M. O., Parrish, R. H., Roy, C., Serra, R., Shust, K. V., Ward, M. N., and Zuzunaga, J. Z.: Worldwide large-scale fluctuations of sardine and anchovy populations, South African Journal of Marine Science, 21, 289–347, https://doi.org/10.2989/025776199784125962, 1999.

895 Segura-Noguera, M., Blasco, D., and Fortuño, J.-M.: An improved energy-dispersive X-ray microanalysis method for analyzing simultaneously carbon, nitrogen, oxygen, phosphorus, sulfur, and other cation and anion concentrations in single natural marine microplankton cells, Limnology and Oceanography: Methods, 10, 666–680, https://doi.org/10.4319/lom.2012.10.666, 2012.

Segura-Noguera, M., Blasco, D., and Fortuño, J.-M.: Taxonomic and Environmental Variability in the Elemental Composition and Stoichiometry of Individual Dinoflagellate and Diatom Cells from the NW Mediterranean Sea, PLOS ONE, 11, e0154 050, https://doi.org/10.
900 1371/journal.pone.0154050, 2016.

Sharp, J. H.: Improved analysis for "particulate" organic carbon and nitrogen from seawater, https://doi.org/10.4319/lo.1974.19.6.0984, 1974.

Sigman, D. M., Altabet, M. A., Francois, R., McCorkle, D. C., and Gaillard, J.-F.: The isotopic composition of diatom-bound nitrogen in Southern Ocean sediments, Paleoceanography, 14, 118–134, https://doi.org/10.1029/1998PA900018, 1999.

Stramma, L., Johnson, G. C., Sprintall, J., and Mohrholz, V.: Expanding Oxygen-Minimum Zones in the Tropical Oceans, Science, 320,
905 655–658, https://doi.org/10.1126/science.1153847, 2008.

Taucher, J., Bach, L. T., Boxhammer, T., Nauendorf, A., Achterberg, E. P., Algueró-Muñiz, M., Arístegui, J., Czerny, J., Esposito, M., Guan, W., Haunost, M., Horn, H. G., Ludwig, A., Meyer, J., Spisla, C., Sswat, M., Stange, P., and Riebesell, U.: Influence of Ocean Acidification and Deep Water Upwelling on Oligotrophic Plankton Communities in the Subtropical North Atlantic: Insights from an In situ Mesocosm Study, Frontiers in Marine Science, 4, https://doi.org/10.3389/fmars.2017.00085, 2017.

910 Teuber, L., Schukat, A., Hagen, W., and Auel, H.: Trophic interactions and life strategies of epi- to bathypelagic calanoid copepods in the tropical Atlantic Ocean, Journal of Plankton Research, 36, 1109–1123, https://doi.org/10.1093/plankt/fbu030, 2014.

van Guelpen, L., Markle, D. F., and Duggan, D. J.: An evaluation of accuracy, precision, and speed of several zooplankton subsampling techniques, ICES Journal of Marine Science, 40, 226–236, https://doi.org/10.1093/icesjms/40.3.226, 1982.

Vervoort, W. and Ramirez, F.: *Hemicyclops thalassius* nov. spec. (Copepoda, Cyclopoida) from Mar del Plata, with revisionary notes on the
915 family Clausidiidae, Zoologische Mededelingen, 41, 195–220, 1966.

Walsh, J. J.: A carbon budget for overfishing off Peru, Nature, 290, 300–304, https://doi.org/10.1038/290300a0, 1981.

Ward, B. B., Kilpatrick, K. A., Renger, E. H., and Eppley, R. W.: Biological nitrogen cycling in the nitracline, Limnology and Oceanography, 34, 493–513, https://doi.org/10.4319/lo.1989.34.3.0493, 1989.

Welschmeyer, N. A.: Fluorometric analysis of chlorophyll a in the presence of chlorophyll b and pheopigments, Limnology and Oceanography, 39, 1985–1992, https://doi.org/10.4319/lo.1994.39.8.1985, 1994.
920

Wiebe, P. and Holland, W.: Plankton patchiness: Effects on repeated net tows, Limnology and Oceanography, 13, 315–321, https://doi.org/10.4319/lo.1968.13.2.0315, 1968.